Title
The Role of Osteocytes in Temporomandibular Joint Diseases

Author
Demirdji, Marianne

Publication Date
2019

Peer reviewed|Thesis/dissertation

The Role of Osteocytes in Temporomandibular Joint Diseases

by
Marianne Demirdji

THESIS
Submitted in partial satisfaction of the requirements for degree of
MASTER OF SCIENCE

in

Oral and Craniofacial Sciences

in the

GRADUATE DIVISION
of the
UNIVERSITY OF CALIFORNIA, SAN FRANCISCO

Approved:

DocuSigned by:
Sunil Kapila
A932A5C7F6B145F...

Sunil Kapila
Chair

DocuSigned by:
Tamara Alliston
DocuSigned by:
Jeffrey Lotz
3D96864A89B54C2...

Tamara Alliston

Jeffrey Lotz

Committee Members

I dedicate this thesis to the animals used for completion of this project.

The Role of Osteocytes in Temporomandibular Joint Diseases

Abstract

Marianne Demirdji

Temporomandibular joint disorders (TMJDs) are a highly prevalent spectrum of conditions occurring in about 6 to 12% of the adult US population totaling over 10 million people and costing billions of dollars in health care and lost productivity. TMJDs frequently present with pain, functional limitations and joint sounds associated with degenerative joint disease, an osteoarthritis (OA)-like condition that significantly affects the quality of life due to its impact on critical functions such as eating and speech. While the etiologies of the temporomandibular joint (TMJ) OA remain unknown, due to the propensity of these disorders in adolescent females- an age group that coincides with orthodontic treatment- orthodontic therapy has often been attributed as a causative or predisposing factor for TMJ OA. Furthermore, severe forms of these disorders such as idiopathic condylar resorption impact on the orthodontist's ability to deliver predictable treatment outcomes. Thus, understanding the causation or predisposing factors for TMJ OA are of critical importance to our profession.

The loss of cartilage extracellular matrix and a compromised subchondral bone are characteristic features of OA of the TMJ. While previous concepts of OA pathogenesis have proposed that cartilage loss is a primary contributor or initiator of OA, more recently it has become clear that cartilage-bone cross-talk are key elements in the pathogenesis of OA. Thus, altered bone quality including its increased or decreased density are known to lead to cartilaginous defects and progression of OA. Bone quality in turn is determined by bone forming and degrading cells including osteoblasts, osteocytes and osteoclasts. Although osteocytes have come to be recognized as key regulators of bone quality, their role in contributing to OA is not currently known. Published data has shown that osteocyte-mediated remodeling is essential for bone and joint health in long bones. More specifically, we have shown that mice with osteocyte specific ablation of matrix metalloproteinase-13 (MMP13), which is involved in perilacunar

remodeling (PLR) by osteocytes have bone quality defects due to collagen disorganization and matrix hypermineralization. However, the role of osteocyte function and osteocyte-mediated bone remodeling in TMJ OA remains unknown. Because OA is a disorder that involves complex and as yet largely unknown cross-talk between cartilage and subchondral bone, we anticipate a potential link between altered bone metabolism through loss of MMP-13 in osteocytes and TMJ OA. Our long-term goal is to understand the contribution of osteocyte-mediated bone phenotypic changes to the progression and severity of TMJ OA by testing the hypothesis that altered PLR through osteocyte-specific knockdown of MMP13 aggravates chemically-induced TMJ OA. Towards this long-term goal, here we performed studies to address the following Specific Aims:

1. Establish and confirm a reproducible and effective method for intra-articular injection of OA-inducing agent, monosodium iodoacetate (MIA) by administration of Fast Green dye.
2. Using data from previous studies on mouse knee joint and rat TMJ, test and establish an effective dose of an OA-inducing agent, monosodium iodoacetate (MIA) that results in OA-like changes in the mouse TMJ.
3. Histologically quantify TMJ health via modified Mankin scoring in WT and MMP13$^{OCY-/-}$ male mice.

Besides providing fundamental information on osteochondral interactions and the role of each of these tissues to the initiation and / or progression of TMJ OA, this study will be important in better understanding the pathogenesis of this disorder and in providing insights into potential therapeutic targets to prevent or alleviate degenerative diseases of the TMJ. Furthermore, determination of an effective MIA dose that generates TMJ OA will establish a mice model for TMJ OA that could be valuable for future studies to identify disease mechanisms.

TABLE OF CONTENTS

LIST OF FIGURES

LIST OF TABLES

CHAPTER 1: INTRODUCTION

1.1. The TMJ in Health and Disease

Temporomandibular Joint Disorders (TMJDs) are a highly prevalent spectrum of conditions occurring in about 6 to 12% of the adult US population totaling over 10 million people and costing billions of dollars in health care and lost productivity. Patients with TMJDs frequently present with facial pain and headaches, joint sounds and functional limitations that significantly affect the quality of life due to its impact on critical functions such as eating and speech. Approximately 10-25% of patients with temporomandibular joint (TMJ) pain demonstrate features of TMJ osteoarthritis (OA).[1,2] TMJ OA is a condition that is classified as low-inflammatory arthritic condition, implying it's chronic and slow onset.[1] Patients with TMJ OA often present with other crippling co-morbidities such as chronic pain and fibromyalgia, and have also been reported to have elevated levels of suicidal ideation, depression, and anxiety as compared to the general population.[3,4] Therefore, new therapies to treat TMJD are clearly needed. While the etiologies of the TMJ OA remain unknown, due to the propensity of these disorders in adolescent females, an age group that coincides with orthodontic treatment, orthodontic therapy has often been attributed as a causative or predisposing factor for TMJ OA.[1,5] Furthermore, severe forms of these disorders such as idiopathic condylar resorption impact on the orthodontist's ability to deliver predictable treatment outcomes. Thus, understanding the causation or predisposing factors for TMJ OA are of critical importance to our profession.

Joint health and optimal function in the TMJ as well as in the appendicular skeleton is a product of healthy articular cartilage, soft connective tissues including ligaments surrounding the joint, and subchondral bone. Defects in any of these can disrupt the crosstalk among these tissue that can lead to disease. Though there is evidence to show that this interaction between the various tissues in the joint are important in joint health and disease, the cellular and molecular mechanisms of this crosstalk are less clear. We have recently found that osteocytes in subchondral bone play a critical causal role in the

progression of joint disease. Specifically, we have found that osteocyte-mediated defects in subchondral bone contribute to the progression of OA of the knee joint (see Chapter 2). Given that the TMJ is a unique joint with distinct developmental origin, composition and function that are different from the knee and other appendicular joints, these findings may not be readily translatable to the TMJ.[6] Therefore, we propose to determine the extent to which defects in osteocyte function contribute to the progression and severity of TMJ OA.

1.2. Contribution of Matrix Metalloproteinases and Perilacunar Remodeling to Joint Degeneration and OA

Matrix metalloproteinases (MMPs) are a family of 25 enzymes that are characterized by their extracellular matrix substrate specificity, zinc-dependent activity, extracellular inhibition by tissue inhibitors of metalloproteinases (TIMPs), secretion as a zymogen and sequence similarities.[7] When MMPs are divided by functionality, MMP13 is identified specifically as a collagenase, with its primary substrates being helical collagens such as types I and II collagen, the predominant collagens found in bone and cartilage, respectively. Osteoblasts and chondrocytes express MMP13 and are directly involved with the degradation of collagen I and II.[2] Indeed, MMP13 expressed by chondrocytes is a key proteinase implicated in cartilage matrix degradation and propagation of OA.[6] In contrast to the known contributions of MMP13 to cartilage matrix loss, the effects of altered levels MMP13 expressed by bone cells particularly osteocytes to OA remains largely unknown. This information is of critical importance due to the fact that altered subchondral bone phenotype is increasingly implicated in contributing to the pathogenesis of OA. Specifically, it has been shown that increased or decreased subchondral bone density leads to secondary adverse changes in overlying cartilage and the perpetuation of OA.[8–10] As bone cells are overloaded in OA, there are extensive changes to the structural framework of the subchondral bone. Some visible features include but are not limited to cartilage thickening, sclerosis, osteophytes, and bone marrow lesions. As the OA progresses, the cartilage layer thickens and becomes increasingly calcified, effectively reducing its primary function of diffusing loads. From these studies, it has been concluded that

the subchondral bone and overlying cartilage effectively function together to promote distribution of mechanical loads. Thus, not only do perturbations in cartilage health induce or aggravate bone degenerative changes, but primary or secondary changes in bone or poor bone quality perpetuate cartilage degeneration.[8,9,11] This interplay between cartilage and bone make the understanding of the effect of one tissue on the other extremely critical to understanding and preventing OA.

In this context, our studies show that the MMP13 ablation results in defective bone matrix organization and impaired bone quality in long bones, defects that we trace to impaired osteocyte function. Similarly, the administration of glucocorticoid represses MMP13 expression in osteocytes in long bones and in the mandible in proximity to defects in bone matrix collagen and mineral organization in the perilacunar regions.[3,12] These lacunae house osteocytes and have a spanning network of canaliculi that have a variety of proposed functions including perilacunar remodeling (PLR).[3] PLR is a process where osteocytes housed in lacunae resorb and replace the local bone matrix to achieve stable systemic mineral levels. The canaliculi off-shooting from the lacunae depend on this remodeling to maintain connectivity of osteocytes to one another and to the vascular supply. In the absence of PLR, there is observed degeneration of the osteocyte lacuno-canalicular network, collagen disorganization, and matrix hypermineralization. Our preliminary analysis of bone from mice with osteocyte-specific MMP13 ablation indicate that cell-intrinsic MMP13 is required for normal PLR and bone homeostasis in long bones (see Chapter 2). However, the consequences and contributions of the resulting changes in bone phenotype to fibrocartilage health and TMJ OA has not been elucidated. Our proposed studies will set the foundation to elucidate the contributions of subchondral osteocytes and bone quality to cartilage degeneration and OA progression in the TMJ.

1.3. Murine Mandibular Anatomy

The mandible develops by intramembranous ossification with the earlier developing Meckel's cartilage serving as a template. Nevertheless the condyle develops endochondrally as a secondary cartilage.[13] This

is of significance because this secondary cartilage of the condyle serves as a growth site for the mandible, whereby chondrocytes proliferate to promote growth. Besides functioning as a growth plate, the condylar cartilage has an articular role that includes responding to functional and masticatory stresses. Following growth, the cartilage remains to continue serving as articular surface for the joint.[14] Additionally, the shape and location of the TMJ changes in murine and human models with age.[15] Liang et al., characterized the development of the murine TMJ from embryonic day 13.5 to post-natal day 180.[16] They characterize TMJ formation over three stages: initiation, growth, and cavitation. The condyle develops upwards into the glenoid fossa with which it articulates. Furthermore, through proliferation and apoptosis that is regulated by a variety of transcription factors and MMPs, the murine condyle develops into the skeletally mature state at the 3-month mark of the animal's life.[16] The posterior portion of the condyle displaces posteriorly – lending to the up and back position of the condyle.[17]

1.4. Methods to induce TMJ OA – particularly Monosodium Iodoacetate (MIA)

MIA has been utilized for osteoarthritis induction for over 20 years, with its effects on joints characterized extensively. Localized injection of MIA into the synovial space of joints in the appendicular skeleton as well as in the rat TMJ results in a cascade of events affecting the function of chondrocytes. The metabolism of chondrocytes is impaired resulting in subsequent cartilage degeneration. Histological analysis has demonstrated this destruction is comparable to that of human OA.[18] While previous studies have used MIA in mediating mice knee joint OA and rat TMJ OA, no information is currently available currently in the dosing and effects of MIA in the mouse TMJ.[2,19–22] We will use the dosing and outcomes data from these studies to test the calculated MIA dose bracket and temporal effects in inducing OA in the mouse TMJ. Current mouse TMJ OA models include dietary models, forced mouth opening, occlusal adjustments, and chemical induction. Dietary models are frequently used and present a non-invasive approach to discerning how changes in mechanical loading alter tissue phenotype. However, varying the pellet hardness (normal diet being hard pellets; experimental being soft) or size is often found to be insufficient in producing degenerative changes in the TMJ.[13] Additionally, the joint changes in this model

are not thoroughly characterized. Forced mouth opening models present an aggressive model to induce TMJ changes which have notable outcomes such as subchondral bone thickening, increased expression of specific genetic markers, and chondrocyte irregularities.[23] However, custom designed springs on mice present logistical issues to maintain the spring, and variations in reproducibility of loading forces. Malocclusion models for TMJ OA such as placement of a unilateral bonded wire to irregularly load the TMJ are not well characterized.[24] Studies using chemical approaches to induction of TMJ OA show reproducible findings, are well-characterized and present a reliable option for TMJ induction.[25] Current approaches include use of complete Freund's adjuvant and MIA. Freund's adjuvant-induced arthritis is highly inflammatory with features similar to that of rheumatoid rather than osteoarthritis.[26] In contrast, the MIA OA model has been used to successfully and reliably induce OA-like disease in rat and rabbit and in the rat TMJ.[2,19–22]

1.5. Summary and Significance

A review of the literature and previously adopted methods led us to use MIA for inducing OA in the mouse TMJ. This required modifying approaches, doses and timelines that have previously been characterized in the mouse knee joint and rat TMJ to establish both the optimal conditions and to effectively administer MIA into the mouse TMJ to result in reproducible TMJ OA. Given the voids in our knowledge on the role of osteocyte-mediated bone remodeling in TMJ OA and because OA is a disorder that involves complex and as yet largely unknown cross-talk between cartilage and subchondral bone, we propose to explore the potential link between altered bone metabolism through loss of MMP13 in osteocytes and TMJ OA. Our overall goal is to understand the contribution of osteocyte-related bone phenotypic changes to the progression and severity of TMJ OA. Because the etiopathogenesis of TMJ OA is poorly understood, current treatments are largely palliative and designed to alleviate symptoms rather than rational and specific approaches to address cause(s) of these disorders. With increasing severity of the disease, it is treated with a spectrum of progressively invasive measures - from observation to full joint replacement. The proposed studies will not only provide fundamental information on osteo-chondral

interactions and the role of each of these tissues to the initiation and / or progression of TMJ OA, but will be important in better understanding the pathogenesis of this disorder and in providing insights into potential therapeutic targets to specifically prevent or alleviate degenerative diseases of the TMJ. For example, if the effect of bone phenotype on fibrocartilage degeneration is demonstrated, then optimal treatment strategies for OA might include targeting both the bone and cartilage compartments. Also, by focusing on the TMJ rather than the hyaline cartilage joints, we will be able to decipher the specifics of fibrocartilage responses to altered bone quality, that will be critical to understanding disease progression that is unique to the TMJ. Thus, the findings will be highly relevant to potential therapies that are specific for TMJ OA.

Previous studies have shown that systemic and osteocyte-specific ablation of MMP13 interferes with PLR in the mouse femur and tibia resulting in altered collagen matrix organization and hypermineralization in the trabecular compartment of long bones.[6] These defects manifest as bone sclerosis and canalicular network degeneration in subchondral bone and exacerbate the severity of joint degeneration in appendicular joints. Specifically, defective PLR results in full-thickness cartilage loss and severe bone sclerosis in the knee joint of MLI mouse model of OA as compared to moderate articular cartilage degeneration in MLI WT mice (see Chapter 2). Though our preliminary data support a causal role for osteocytic PLR in appendicular joint disease, the extent to which proteinases involved PLR such as MMP13 play a causal role in TMJ OA remains to be determined. Equally importantly, while we show the adverse effect PLR defects in subchondral bone on hyaline cartilage joint, it is not yet clear how these boney changes impact the progression of TMJ OA. Therefore, to evaluate the causal role of PLR in TMJ OA, we performed initial studies to evaluate the TMJ OA phenotype in $MMP13^{OCY-/-}$ mice in the MIA model using the optimal dose conditions.

CHAPTER 2: PREVIOUSLY PUBLISHED MATERIALS

2.1. PLR is Controlled by Regulating Essential PLR Enzymes

Osteocyte specific MMP13 null mice that will be used in these studies have been used to generate important preliminary data that points to the potential role of PLR in TMJ OA. The importance of osteocyte-mediated PLR in health and disease has been characterized by studying the effects of enzymes that regulate bone remodeling on this process. Several osteocyte derived proteins have been implicated in PLR including cathepsin K, MMP13, MMP14, MMP2, TRAP, carbonic anhydrase 2, and the Na/H+ exchanger.[12] Deficiency in each of these key enzymes impairs canalicular networks and yields other hallmarks of defective PLR. More specifically, dysregulation of bone remodeling caused by systemic or osteocyte-specific ablation of MMP13 significantly compromises bone quality (Figure. 2.1). This includes aberrant collagen organization, hypermineralization and decreased resistance to fracture.[12]

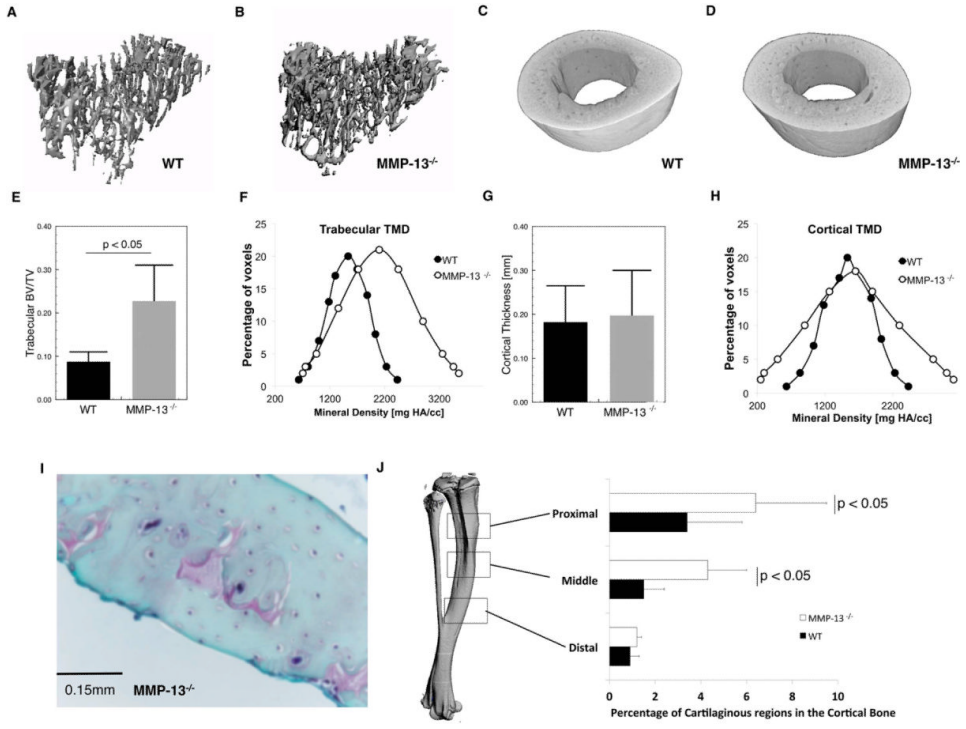

Figure 2.1. MMP-13-deficiency results in increased trabecular bone volume and the altered distribution cortical bone mineralization. The trabecular bone contoured from the proximal region of the tibia confirms previous observations that MMP13$^{-/-}$ bones have significantly increased trabecular bone volume fraction (BV/TV; $p < 0.05$) (A, B, E, F). MMP13-deficiency did not affect the geometric structure of the cortical bone (cortical thickness; $p = 0.52$) (C, D, G). Nonetheless, a histographic plot of the cortical bone

tissue mineral densities (Cortical TMD) reveals that MMP13 $^{OCY-/-}$ mice have significantly altered TMD distribution ($p < 0.001$), characterized by an increased incidence of lower and higher TMD compared to the WT (H). This can in part be explained by the osteoid remnants, which stain red with Safranin-O, that are predominantly observed in the middle and proximal aspects of the tibia (I). However there were no detectable differences in Safranin-O staining in the distal region near the tibiofibular junction where bulk of the subsequent analyses were performed (J).

2.2. PLR is suppressed in human joint disease

Although the abnormal subchondral bone of post-traumatic OA (PTOA) and osteonecrotic joints has been well-described, the integrity of PLR in these conditions has not previously been known.[27–29] We found that subchondral bone from patients with PTOA and osteonecrosis exhibits each of the classical hallmarks of defective PLR. Femoral head subchondral bone from patients with glucocorticoid- induced osteonecrosis has reduced levels of MMP13, disorganized collagen, truncated canaliculi, smaller lacunae, and hypermineralization (Figure 2.2). Our preliminary data indicate that the same hallmarks are present in PTOA tibial plateaus from veterans receiving knee replacements.[3] Among these, the most compelling evidence of PLR suppression is that canalicular length is reduced by 56% in PTOA bone, relative to bone from non-PTOA cadaveric donors (Figure 2.3, p=0.003**)**. Furthermore, canaliculi on the medial side of the tibial plateau, the most common site of PTOA, appear to be shorter than those on the relatively healthier lateral side of the same joint. Collectively, our findings strongly support the conclusion that PLR is suppressed in human osteonecrosis and in PTOA. However, analysis of tissues with terminal disease does not clarify whether PLR suppression contributes to disease progression, or is a result of the disease process. Thus, there is substantial value to performing *in vivo* mechanistic studies to understand the temporal relationship between PLR and OA and the direct contributions that aberrant PLR makes to OA.

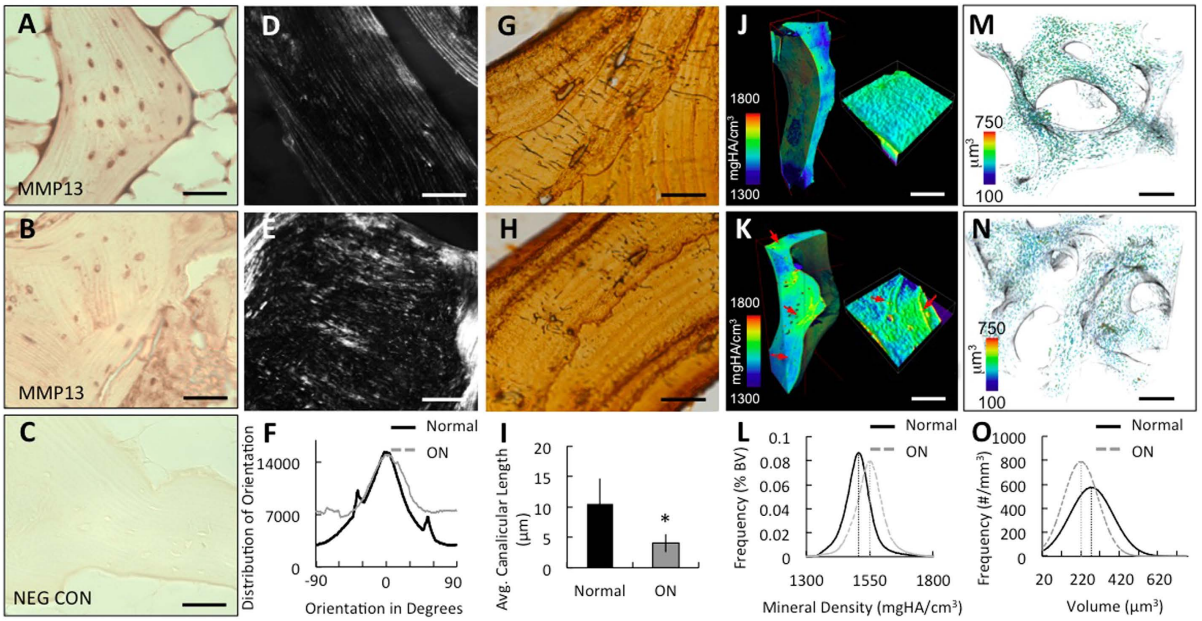

Figure 2.2. PLR suppression in human osteonecrosis. Trabeculae from the sclerotic regions of human femoral heads (B,E,H,K,N) show hallmarks of defective PLR relative to those distant from the lesion (A,D,G,J,M). These include reduced MMP13 expression (IHC, A–C) (scale bar, 20 µm), defects in collagen organization (picrosirius red stain, D–F) (scale bar, 50 µm), and reduced canalicular length (silver nitrate stain, G–I). Bar graph represents mean ± SEM of $n \geq 3$ regions from human cadaveric or human osteonecrotic bone samples, * p-value ≤ 0.05 compared to control. Xray tomographic microscopy shows hypermineralization (L, red arrows) and reduced lacunar size (O) in osteonecrotic bone (K,N) relative to trabeculae that are more distant (J,M). Vertical lines (L,O) signify peak volumes.

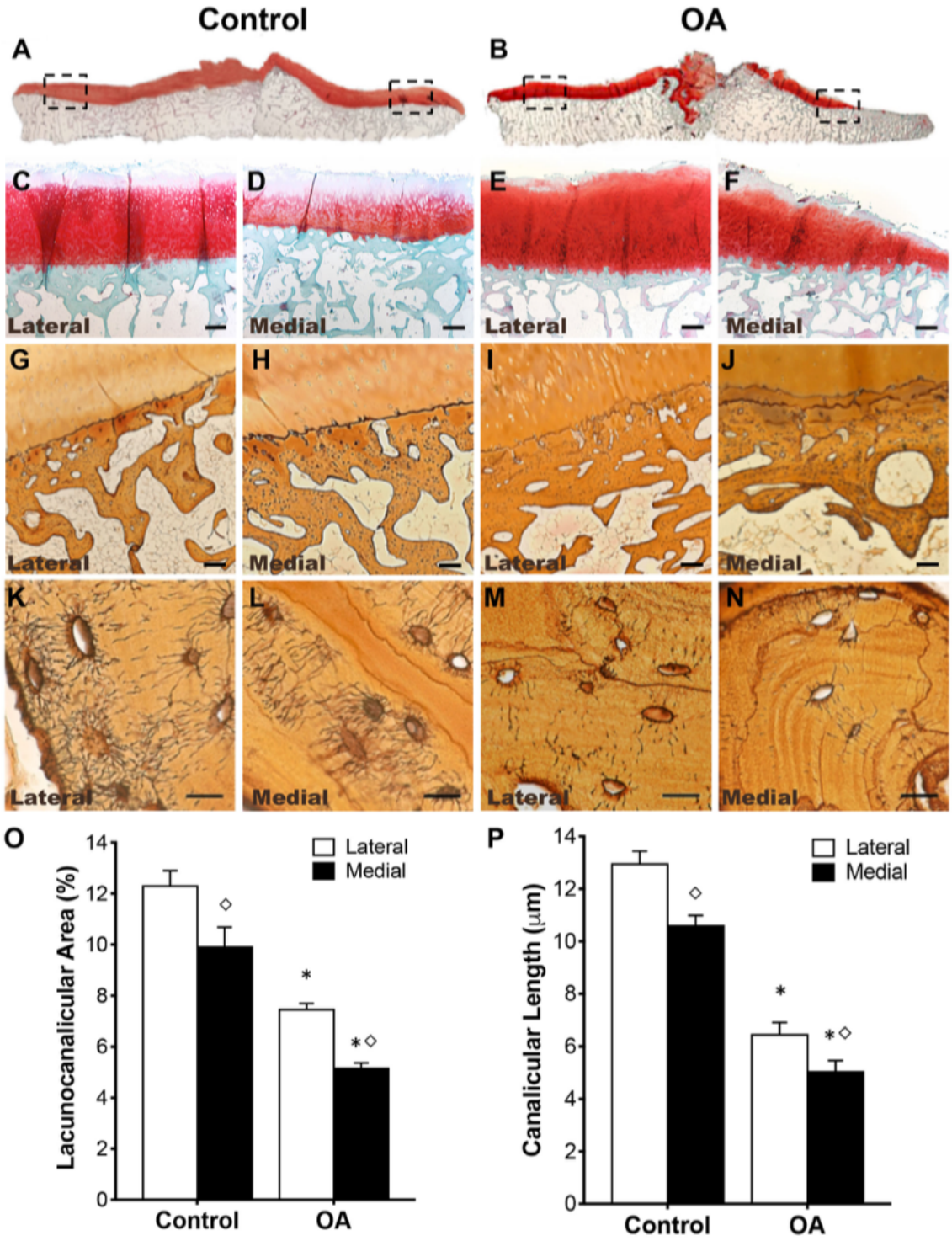

Figure 2.3. Disrupted lacunocanalicular networks in human OA subchondral bone**.** Control cadaveric (A, C, D) and OA (B, E, F) specimens stained with Safranin-O/ Fast Green and imaged at 0.5x (A, B) or 10x (C-F) magnification displayed differences in articular cartilage and subchondral bone morphology on the

lateral and medial sides of the tibial plateau. Subsequent analyses compared the indicated regions of interest (black boxes in A, B) between control and OA specimens, and between the less affected lateral side with the more severely degraded medial side. These identified regions of interest in Ploton silver stained sections were evaluated at low (4x, G-J) and high (100x, K-N) magnification to visualize the lacunocanalicular network of subchondral bone. Quantification of lacunocanalicular area normalized to bone area (O) and canalicular length (P) revealed significant OA-dependent reductions in both parameters (n=5). Scale bars are 400 μm in C-F, 200 μm in G-J, and 20 μm in K-N. *$p<0.05$ compared to respective regions of control specimens, $p<0.05$ between regions by Holm-Sidak post-hoc tests.

2.3. PLR suppression compromises subchondral bone quality and plays a causal role in PTOA

In addition to our findings on effects of dysregulated PLR on trabecular bone in long bones, we have found sclerotic bone and abrogated canalicular networks (Figure 2.4) in subchondral bone in mice with either systemically ablated MMP13, or with osteocyte-specific knockout of MMP13.[12] Our preliminary data further support the causal role of PLR suppression in joint disease. Using an established medial collateral ligament (MLI) injury model of knee joint PTOA in which the medial collateral ligament is transected and the medial meniscus is removed, we tested the hypothesis that PLR suppression would exacerbate the severity of PTOA.[30,31] While the analyses are still underway, the preliminary data support this hypothesis. Relative to the anticipated moderate degeneration of articular cartilage in MLI wild-type mice Figure 2.5B, the degeneration in an osteocyte-intrinsic model of PLR suppression (TBRII $^{OCY-/-}$) demonstrated full-thickness cartilage loss and severe bone sclerosis as visualized histologically (Figure 2.5D). These findings support and extend the conclusions derived from the osteonecrosis model, in which glucocorticoid excess affected multiple cell populations. Specifically, we find that osteocyte-intrinsic suppression of PLR is sufficient to exacerbate the severity of joint degeneration. The extent to which similar processes participate in the degeneration of the TMJ remain to be determined and are the focus of this study.

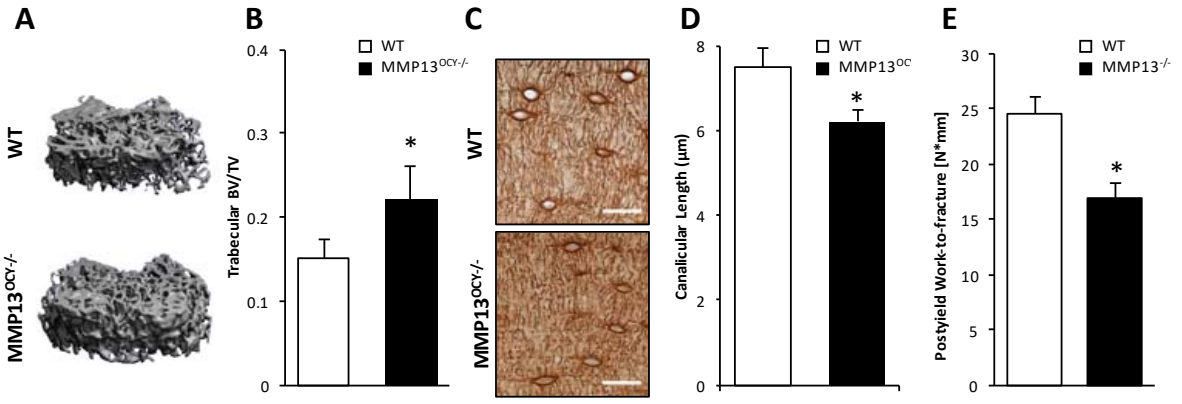

Figure 2.4. Osteocyte-intrinsic ablation of the PLR enzyme MMP13 causes subchondral bone sclerosis and canalicular network degeneration. Osteocyte-specific ablation of MMP13 results in trabecular bone sclerosis (A,B) and reduced canalicular length (silver nitrate stain, C,D). These findings complement those in human PTOA and in systemic MMP13-deficient mice, which also show poor bone quality with significantly reduced work- to-fracture (E). * p-value ≤ 0.05 compared to control.

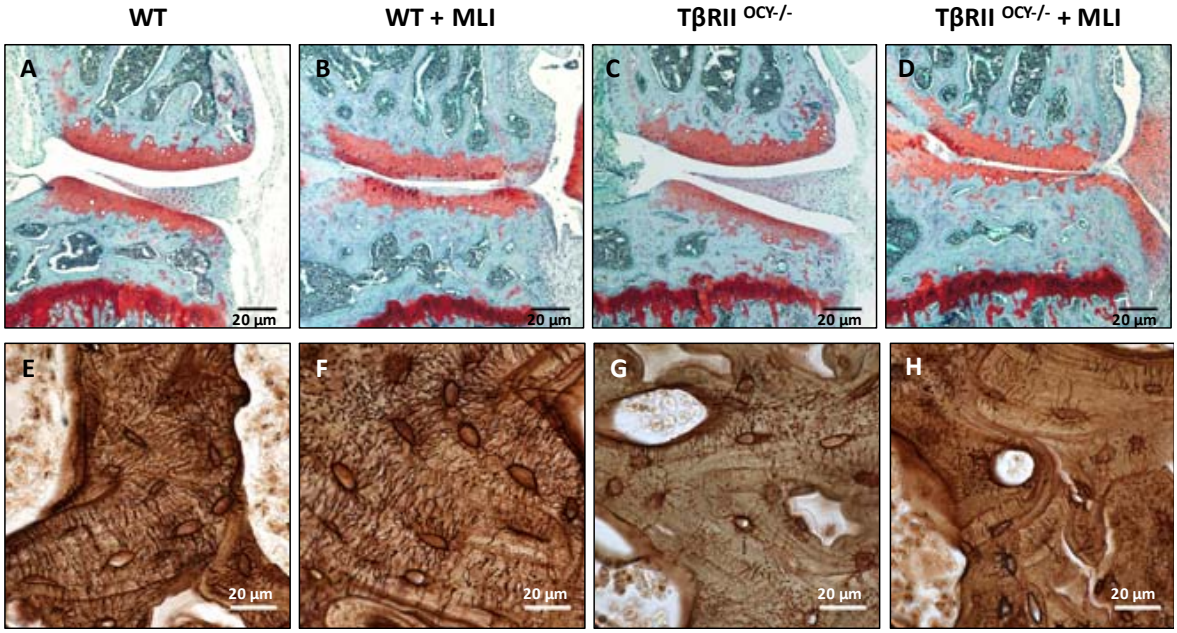

Figure 2.5. Increased PTOA severity in TβRIIOCY-/- mice shows critical role of osteocytes in joint disease. Meniscal/ligamentous injury (MLI) in WT mice results in a PTOA phenotype with loss of proteoglycan staining and subchondral bone sclerosis (Safranin- O/Fast Green stain, B) compared with non- injured controls (A) (scale bar = 20 µm). Defective PLR, induced by osteocyte-specific ablation of TβRII, exacerbates cartilage degeneration and subchondral bone sclerosis in the presence of injury (D) compared with uninjured TβRII $^{OCY-/-}$. Canalicular networks are disrupted in TβRII $^{OCY-/-}$ mice (G, H) compared with WT mice (E,F). Blinded reviewers consistently ranked the joints of the MLI TβRII $^{OCY-/-}$ mice as the most severe PTOA phenotype. This qualitative preliminary data is representative of N=5 mice/group.

2.4 Experiments to Induce TMJ OA and Assay TMJ Degeneration

Our lab (Kapila et al., 1995) has previously developed and characterized the first reproducible animal model of inflammatory TMJ disease and were also the first to document the mandibulofacial growth changes in juvenile rheumatoid arthritis (JRA)-like disease of the TMJ in this animal model.[26] We have also characterized the MMPs expressed by TMJ cells, which provided the foundation of subsequent work by several investigators in deciphering the TMJ disease progression and markers of disease.[32] The preliminary data provided below demonstrates the technical and intellectual know-how to conduct the studies proposed in this application, which include histochemical and biochemical assays on changes in cartilage matrix macromolecules (Figure. 2.6) and μCT analyses of subchondral bone porosity (Figure 2.7).

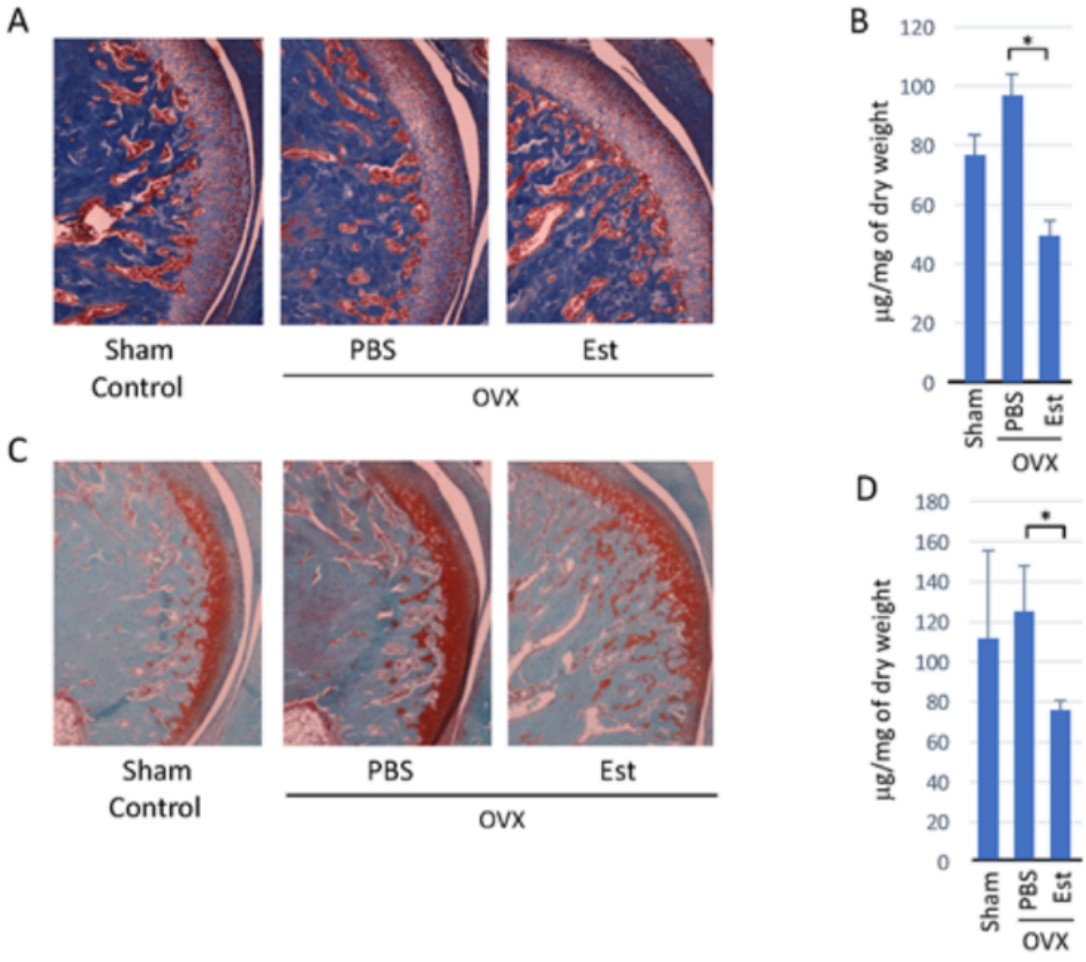

Figure 2.6. In Vivo Effects of Estrogen (Est) on Collagen and Glycosaminoglycan (GAG) content of TMJ Fibrocartilage. Ovariectomized (OVX) young female mice were administered PBS or estrogen for seven days and TMJ or fibrocartilage harvested for histochemical staining (A and C) or biochemical assays for collagen (B) or GAG (D), respectively. (A) Masson's trichome staining showing diminished collagen staining (blue) in TMJ fibrocartilage from estrogen treated mice relative to controls, that corresponds with loss of collagen as determined by hydroxyproline assay (B). (C) Safranin-O staining demonstrates decreased staining for GAG (orange) in TMJ fibrocartilage from estrogen treated mice relative to PBS control mice, which is confirmed quantitatively by Alcian Blue assay (D). Sham-operated mice were used as controls ($P < 0.05$).

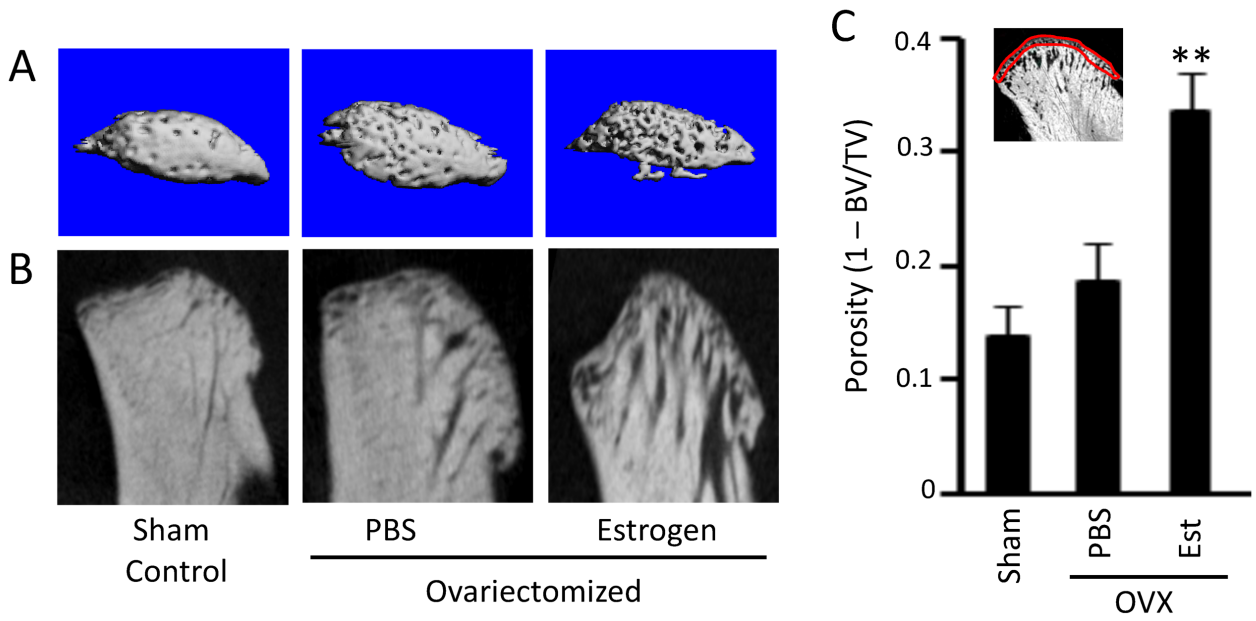

Figure 2.7. In Vivo Effects of Estrogen (Est) on Subchondral Bone Porosity**.** Ovariectomized (OVX) young female mice were administered PBS or estrogen and TMJs retrieved for microCT after 28 days. Three-dimensional reconstruction (A) and coronal sections (B) of representative condyles show increased subchondral porosity. (C) This finding was confirmed quantitatively by analyzing the porosity in the subchondral zone (demarcated by the red line in the panel) and found to be statistically significant in mice administered estrogen relative to sham and PBS control mice (**P < 0.01).

CHAPTER 3: EXPERIMENTAL DESIGN AND METHODS

3.1. Selected Mice and Allocated Groups

A power analyses (see Statistical Analyses) indicates that a sample size of 4 specimens per group will result in a statistical significance at the 0.05 level (two-tailed). Statistical analyses on the effects of MIA on OA severity and other quantitative data will be performed as described below (see Statistical Analyses). Mice were generated by breeding homozygous MMP13-floxed mice that possess loxP sites flanking exons 3, 4, and 5, which encode the enzyme's active site with hemizygous -10kb-DMP1-cre$^{+/-}$ mice, which express Cre recombinase primarily in osteocytes.[33,34] Half of the mice from the resulting cross were DMP1-Cre$^{+/-}$; MMP13^{flfl} (named MMP13 $^{OCY-/-}$) and half were DMP1-cre$^{-/-}$; MMP13$^{fl/fl}$ littermate controls (named WT mice), as confirmed by PCR genotyping. All experiments were initiated on 12-week old mice using animal procedures approved by the Institutional Animal Care and Use Committee of the University of California San Francisco and the Indiana University School of Medicine. Once determined, the final injection protocol was practiced until sufficient competence was achieved for establishment of the injection protocol as proposed in Aim 1. Mice used for dose determination in Aim 2 was allocated as follows: four mice for the 0.10 mg (4 mg/kg) MIA dose, two for the 0.05 mg (2 mg/kg) MIA dose, and 3 for the saline group due to time constraints and limitations in animal availability. While this is insufficient to draw conclusions due to a lower power and sample size, conclusions can be drawn from the preliminary analysis to allow for further studies. In order to compare 28 day male WT vs MMP13$^{OCY-/-}$ as described in Aim 3, five samples were obtained per group. Representative male and female samples at 7 and 28 day WT and MMP13 $^{OCY-/-}$ were also collected for future studies and are displayed in Figures 9-11.

3.2 TMJ Injection Protocol

In order to establish a proper injection protocol, a variety of needle gauges, lengths, and paths of injection were attempted. A 30 gauge needle was determined to not effectively pierce the mouse tissue. From this a

25 gauge needle was used to effectively pierce through the mouse tissue. Differing lengths of needles were used and eventually decided based of efficacy of delivery. The influencing factors for this decision were the length of the mouse from the TMJ to the nose tip as well as the volume of the fluid to be injected to the TMJ. A 25 gauge 0.625 inch was eventually used for all injections. Differing angulations of injection were also tried which are detailed in the Discussion. The final chosen injection method was to insert and place the needle parallel to and directly inferior to the zygomatic arch, as medial as possible. The needle lies directly parallel to the mouse head. The needle is then inserted until it hubs against nose of mouse and lateral to mouse molars as shown in Figures 3.1A and 3.1B. When the needle hubs, the tip is nearly flush with cochlea.

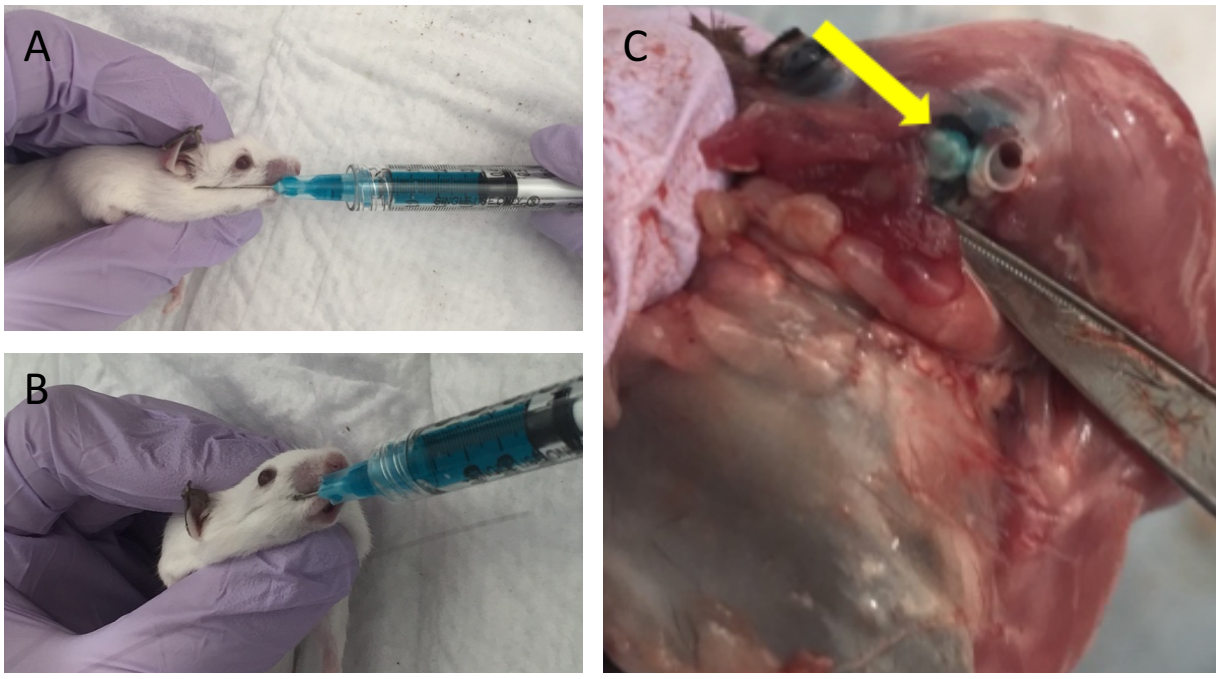

Figure 3.1. Injection into the TMJ. Characterizing and verifying an optimal method for intra-articular TMJ injection in the mouse. Lateral (A) and anterior (B) views showing direction of needle insertion. (C) Dissected mouse head showing Fast Green staining of condylar head and TMJ fossa (arrow).

3.3 Procedure for Aim 1

12 week old mice allocated for Aim 1 were euthanized post-injection via lethal dose of CO_2, followed by cervical dislocation. Intra-articular administration of Fast Green dye was confirmed by TMJ dissection as

demonstrated in Figure 3.1C. These procedures were modified as needed and repeated until injections were noted to deposit the dye into the joint as desired for future injections. Once an optimal method was identified, these experiments were repeated in anaesthetized mice to confirm the adequacy of this technique

3.4 Procedure for Aim 2

The TMJ OA was induced by injection of MIA dissolved in 10 µl saline into both TMJs of 12-week old mice using a 25 gauge 0.625 inch needle under anesthesia without surgical assistance. In establishing and characterizing OA TMJ model in mice, we performed preliminary dose-response analysis of the effects MIA administered into mouse TMJs. Using dose data from previous studies on MIA-induced OA in mouse knee joint and rat TMJ adjusted by joint volume and weight, respectively, we calculated a low and high range of MIA dose and optimal volume to use in the mouse TMJ.[20,21,25,35] These calculations indicated a low MIA dose of 0.05 mg (2 mg/kg) and high MIA dose of 0.10 mg (4 mg/kg) in saline should generate reproducible OA in the mouse TMJ. Similarly, these studies have demonstrated joint changes characteristic of OA within 3 to 21 days of intraarticular administration of MIA.[20,21,25,35] Thus using a small sample of mice and 10 µl of PBS or low (0.05 mg) or high (0.10 mg) dose of MIA we histologically assayed mice at 28 days following administration of MIA or PBS. Un-injected control animals did not receive anesthesia or analgesics. All animals were allowed unrestricted activity, food, and water. At 28 days post injection (dpi), animals were euthanized via lethal dose of CO_2, followed by cervical dislocation and hemi-mandibles were harvested for histological and radiographic analyses. The left hemi-mandible were frozen for future µCT studies. The right hemi-mandible was fixed overnight in 4% paraformaldehyde, decalcified, sectioned, stained with Safranin-O/Fast Green stain and OA severity determined through modified Mankin scoring.

3.5 Procedure for Aim 3 and representative samples

Since OA studies will be performed at 7 and 28 following injection of MIA in 12-week old mice, for this part of the study, we analyzed tissues from representative control mice 13 weeks (controls for 7 dpi mice) and 16 weeks (controls for 28 dpi mice) of age. Representative samples at these time points for male and female WT and MMP13 $^{OCY-/-}$ were collected. Of these five samples each from WT and MMP13$^{OCY-/-}$ 16-week old male mice (controls for 28 dpi) were analyzed per group for the current studies while the rest were banked for ongoing studies. Un-injected animals did not receive anesthesia or analgesics. All animals were allowed unrestricted activity, food, and water. Mice were euthanized via lethal dose of CO_2, followed by cervical dislocation.

3.6 Histology and OA Quantitation

The hemi-mandibles were dissected and fixed in 10% neutral buffered formalin and then decalcified in 10% EDTA until fully decalcified, followed by serial ethanol dehydration and paraffin embedding. Coronal sections (6 μm thick) were generated using a microtome (Leica Microsystems, Buffalo Grove, IL) for Safranin-O/Fast Green stain.

Safranin-O with Fast Green protocol was adapted from University of Rochester (University of Rochester Center for Musculoskeletal Research. Safranin O/Fast Green stain for Cartilage. https://www.urmc.rochester.edu/musculoskeletal-research/core- services/histology/protocols.aspx. Published 2017. Accessed May 1, 2018). Briefly, paraffin sections were deparaffinized, rehydrated, and stained in Weigert's Iron Hematoxylin for 5 minutes then washed in water and differentiated in 1% acid-alcohol. Slides were then incubated in 0.02% Fast Green for 15 minutes, followed by staining with 1.0% Safranin-O for 20 minutes and subsequently dehydrated, cleared, and mounted. Images were captured using a Nikon Eclipse E800 bright-field microscope for OA quantitation.

A minimum of three sections of each condyle taken as close as possible to the midcoronal location of the joint were used to quantitate OA using modified Mankin score that is scored from 0 (normal cartilage) to 14 (aggressive cartilage destruction) as shown in Table 3.1. [36,37]

Table 3.1. Modified Mankin Score used to characterize osteoarthritis severity[37]

Cartilage Erosion Scoring (CES)	
Smooth non-eroded Cartilage	0
Rough non-eroded Cartilage	1
Superficial fibrillation	2
Separation of uncalcified from calcified cartilage	3
Erosion of uncalcified cartilage only	4
Erosion extending into calcified cartilage	5
Erosion down to subchondral bone	6
Chondrocyte periphery staining (CPS)	
Normal	0
Slightly decreased	1
Intensely decreased	2
Spatial arrangement of chondrocytes (SAC)	
Normal	0
Diffuse hypercellularity	1
Clustering	2
Hypocellularity	3
Background staining intensity (BSI)	
Normal	0
Slight reduction	1
Moderate reduction	2
Severe reduction	3
No dye noted	4

3.7. Statistical Analyses and Data Management

Sample Size Calculations: Power analysis was performed using conservative assumptions and based upon data from prior studies by our group and others. This analysis indicates an 80% chance of reaching statistical significance at the 0.05 level (two-tailed) with a sample size of 4 specimens per group. q1 = 0.500 [MMP13$^{OCY-/-}$ mice with TMJ OA]; q0 = 0.500 [DMP1 mice with TMJ OA]; Alpha = 0.05 (2-sided); Beta = 0.20 (80% power); E = 1.3 - 0.5 = 0.80; S = 0.4. Five WT and five MMP13 $^{OCY-/-}$ mice at 16 weeks old were analyzed to assess for differences in OA severity. Histologic analysis was performed using the modified Mankin OA score. The panels of images were scored by 3 independent blinded graders. Scores were summed and averaged. These scores were used for the descriptive and statistical purposes. Data was

analyzed using Excel software with an unpaired two sample and two tail t-test with the assumption that the data is normally distributed.

CHAPTER 4: RESULTS

4.1 Selected Method of Intra-articular Injection

Due to the size of the mouse TMJ we used a 25 gauge 0.625 inch needle for all injections. After several trials we identified the optimal method of injections. This involved placing the needle parallel to and directly inferior to the zygomatic arch, as medial as possible relative to the nasal midline. With the needle lying directly parallel to the mouse head in a sagittal direction, it is the inserted into the skin until it hubs against nose of mouse and lateral to mouse molars. The solution is deposited within the glenoid fossa of the articulating TMJ condylar head.

4.2 Histological Observations in Un-injected Control Mice

Figures 4.1-4.3 demonstrate representative samples of mice from groups of either WT or MMP13$^{OCY-/-}$, male and female mice at 13 weeks old (7 dpi controls) or 16 weeks (28 dpi controls). Statistical analyses were not conducted on these animals since each group is presented with a representative sample of n = 1. The females on average appear to have a slightly smaller width of Safranin-O staining in comparison to the males. The females additionally show slightly greater amount of Safranin-O staining throughout the neck of the condyles as compared to the males. Males generally show greater cellular disorganization that the females. Additionally, although there are shape differences in the condyles across the panels, this can be attributed to differences in sectioning protocol. However, female 28 dpi demonstrates significant flattening and shape irregularities as well as thinness of Safranin-O staining region.

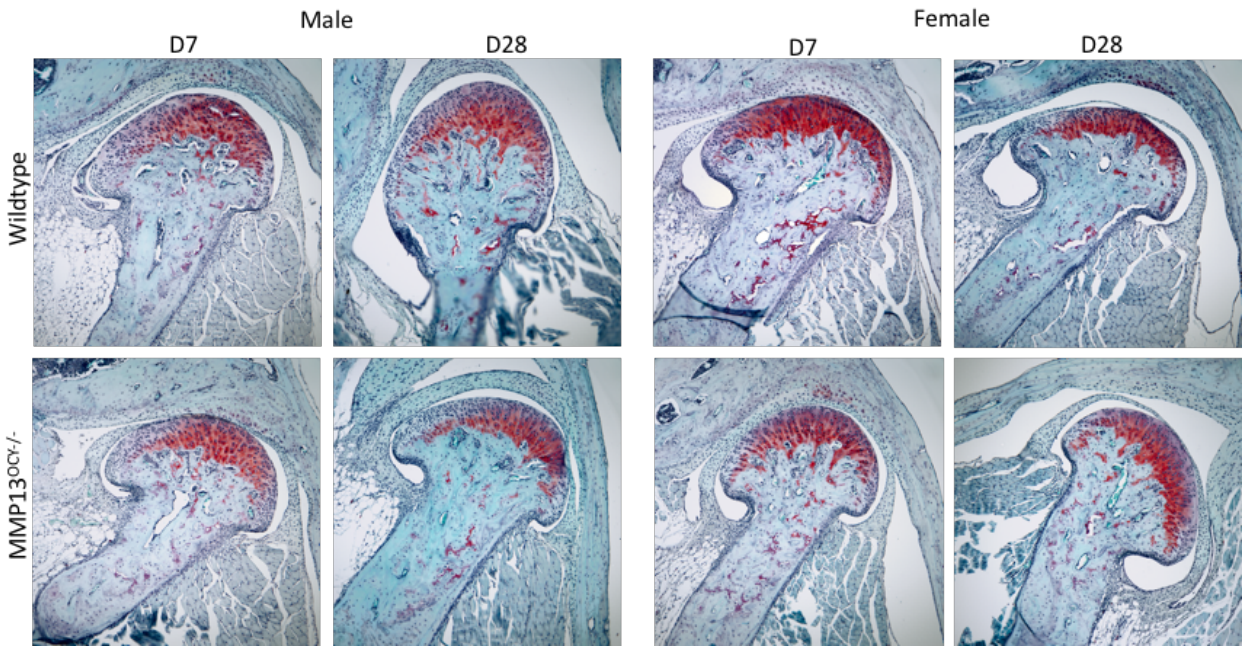

Figure 4.1. Coronal sections of male versus female WT and MMP13$^{OCY-/-}$ TMJ at 13 weeks (7 dpi controls) and 16 weeks (28 dpi controls) with Safranin-O/Fast-green stain at 10x (un-injected controls)

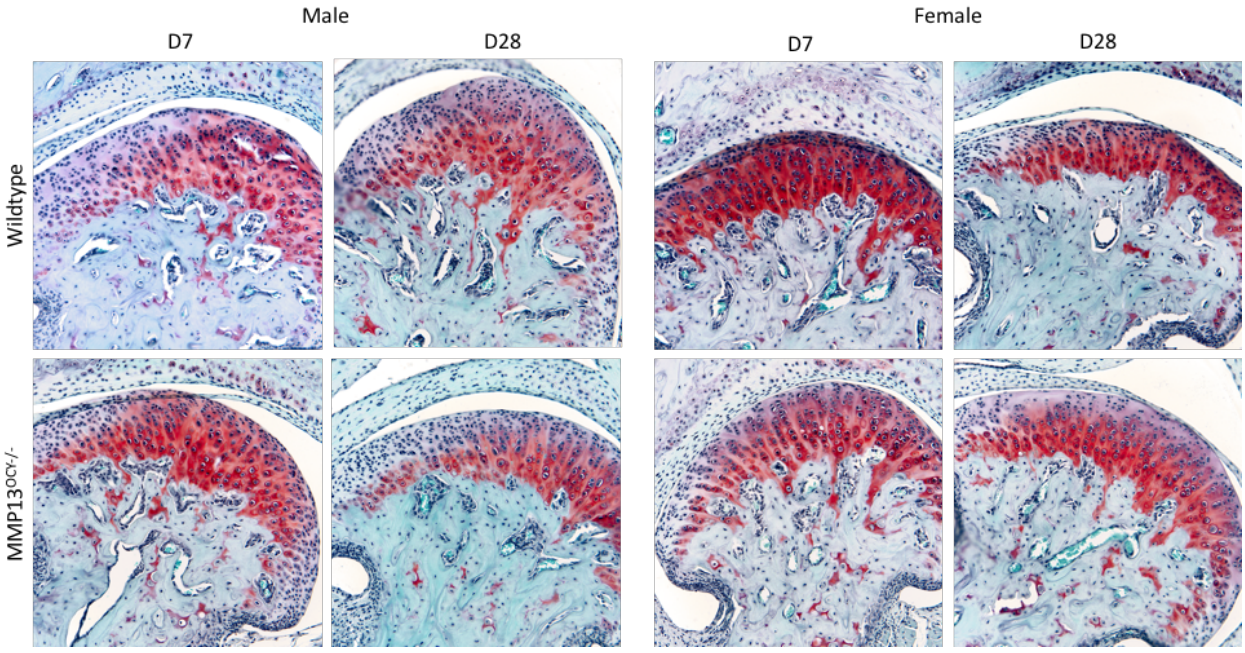

Figure 4.2. Coronal sections of male versus female WT and MMP13$^{OCY-/-}$ TMJ at 13 weeks (7 dpi controls) and 16 weeks (28 dpi controls) with Safranin-O/Fast-green stain at 20x (un-injected controls)

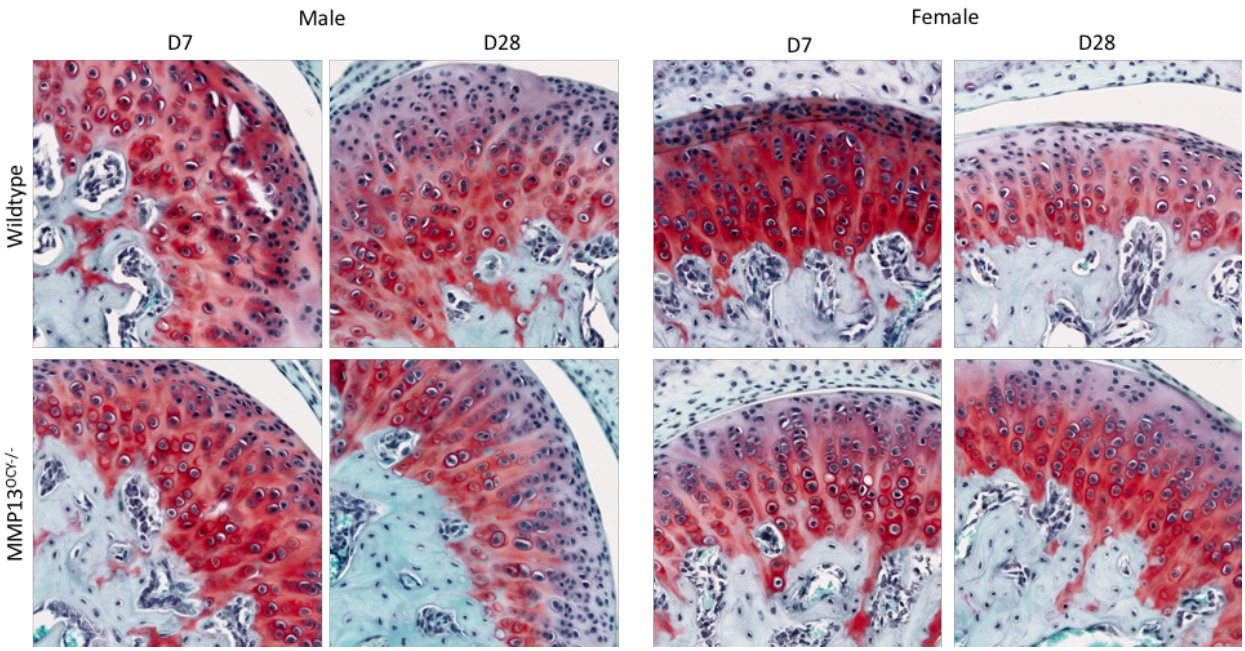

Figure 4.3. Coronal sections of male versus female WT and MMP13$^{OCY-/-}$ TMJ at 13 weeks (7 dpi controls) and 16 weeks (28 dpi controls) with Safranin-O/Fast-green stain at 40x (un-injected controls)

4.3 Effects of MIA on Induction of OA in the TMJ

Figures 4.4 to 4.6 demonstrate coronal sections of saline versus MIA injected TMJs in WT mice at 28 dpi three different magnifications. Each panel represents a different animal. The first panel for 0.10 mg MIA dose demonstrates significant loss of cellularity and staining (black arrow) just above the subchondral bone. Slight loss of cellularity is also observed in first panel for 0.05 mg MIA dose (yellow arrow). A differential gradient of staining is observed for all samples. There is less Safranin-O staining with MIA than saline which appears to be more substantial with 0.1mg MIA than 0.05mg MIA. This is similarly exhibited for cellularity.

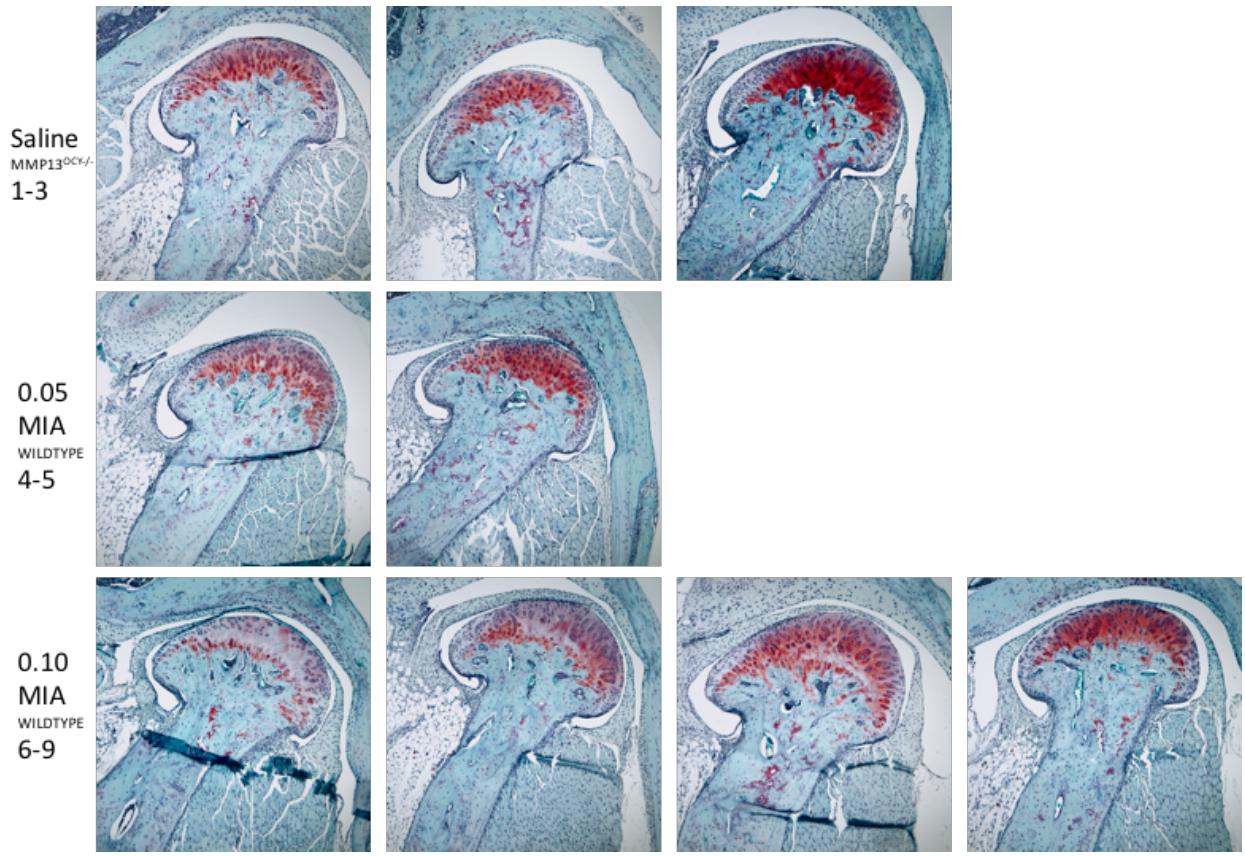

Figure 4.4. Coronal sections of TMJs from control PBS MMP13OCY$^{-/-}$ vs 0.05 mg MIA WT and 0.10 mg MIA WT mice at 28 dpi (10x magnification)

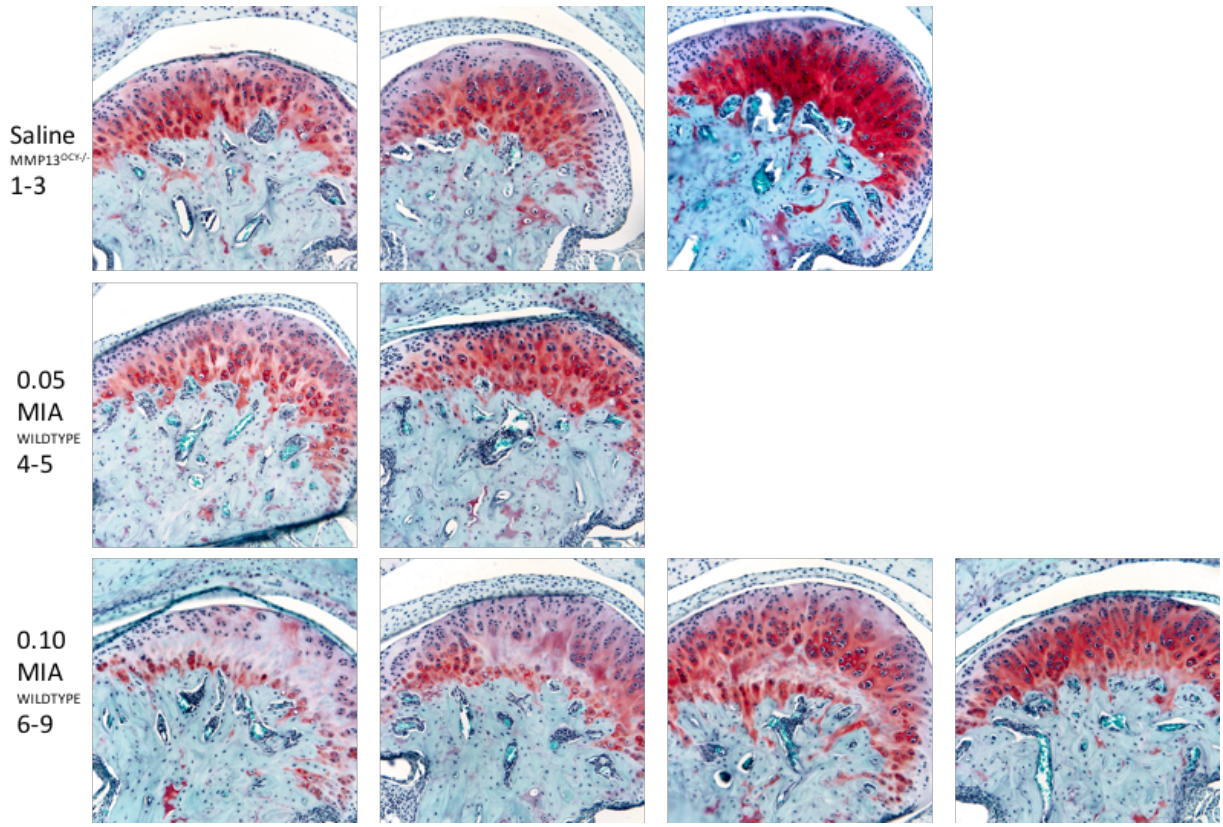

Figure 4.5. Coronal sections of TMJs from control PBS MMP13OCY$^{-/-}$ vs 0.05 mg MIA WT and 0.10 mg MIA WT mice at 28 dpi (20x magnification).

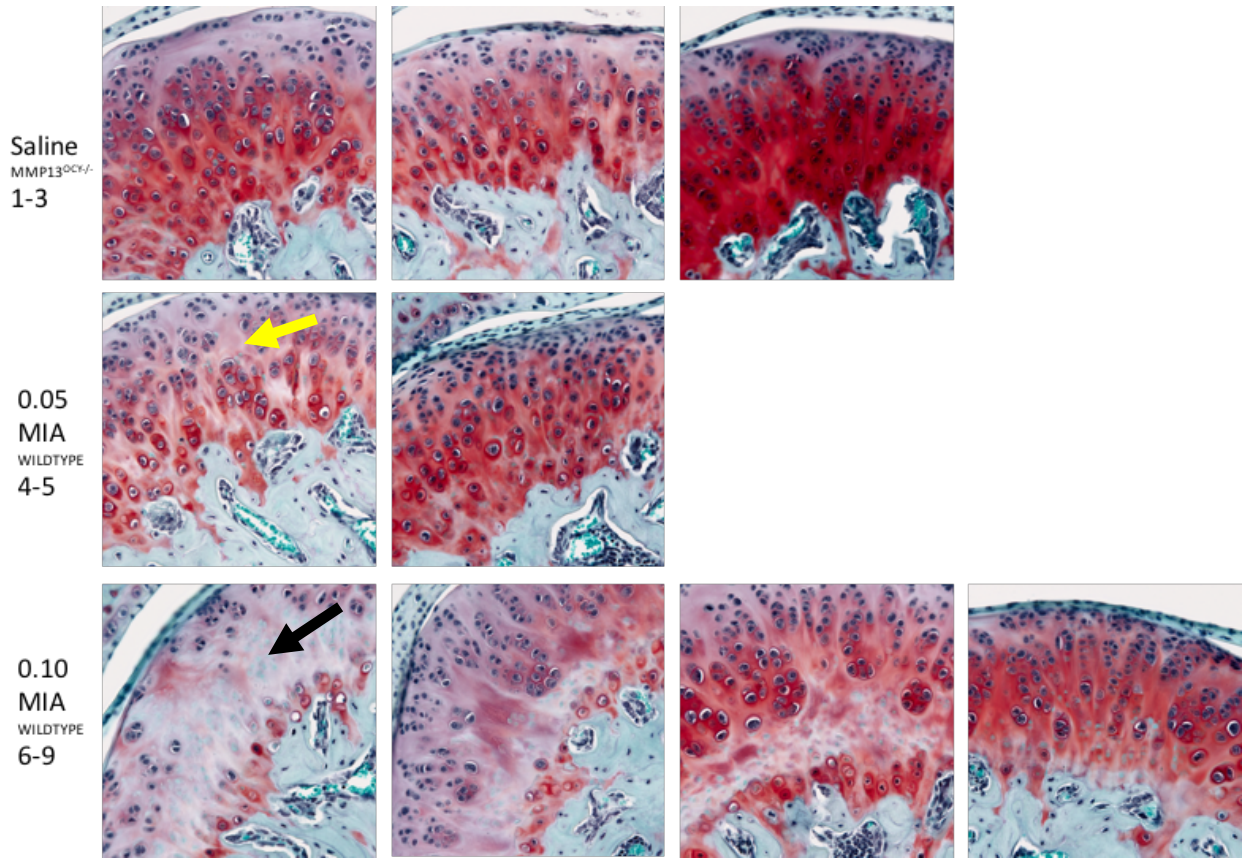

Figure 4.6. Coronal sections of TMJs from control PBS MMP13OCY$^{-/-}$ vs 0.05 mg MIA WT and 0.10 mg MIA WT mice at 28 dpi (40x magnification).

The sample was quantified by Mankin scoring, but due to the lack of power for this group, statistical analyses was not performed. The modified Mankin scoring demonstrated that MIA at 0.10 mg dose appeared to have higher scores in all categories apart from cartilage erosion scoring. MIA at 0.05 mg dose was second highest in scoring again in all categories apart from cartilage erosion scoring. Cartilage erosion scoring shows the most variable results in comparison to all other OA features.

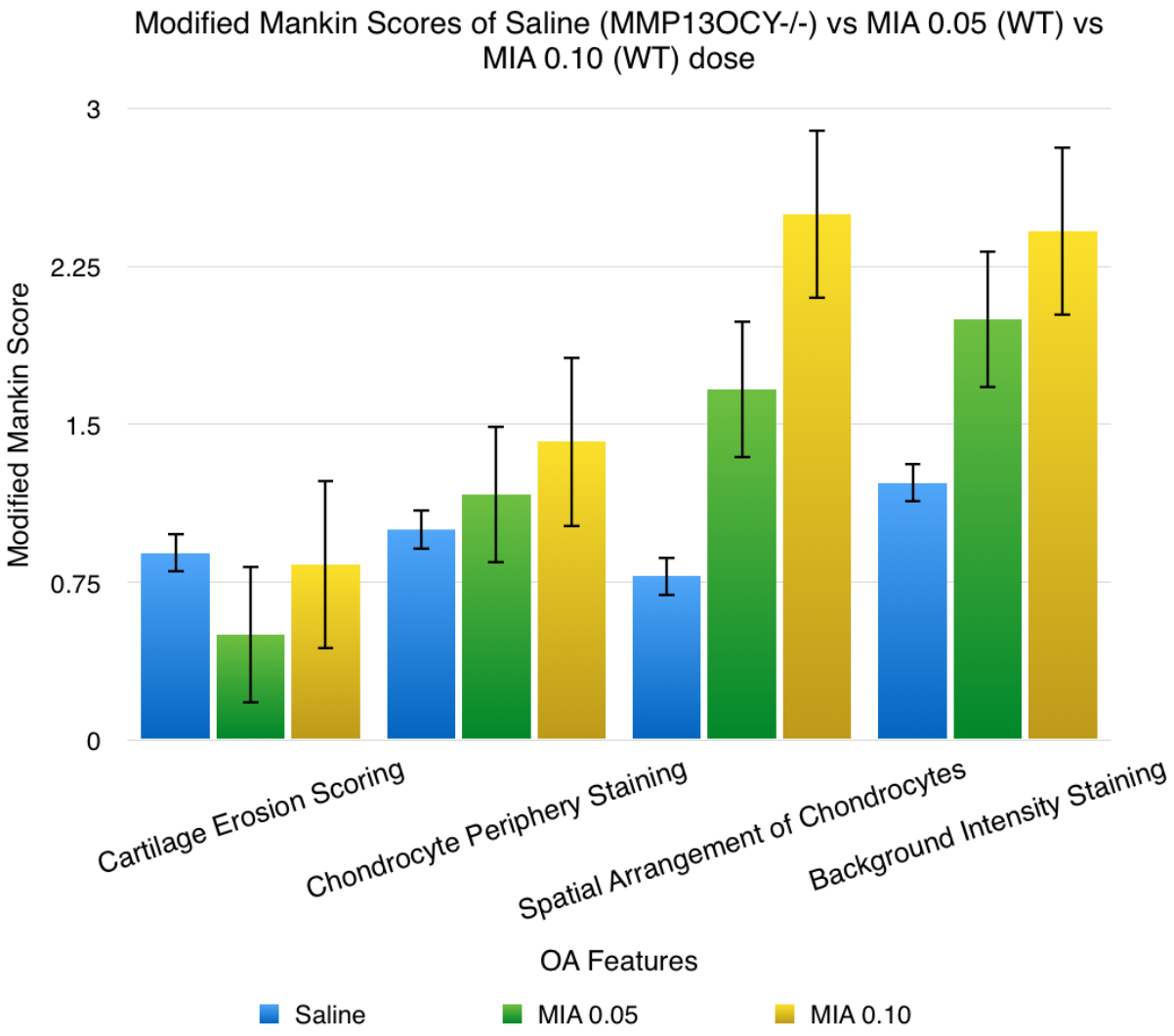

Figure 4.7. Modified Mankin Scores of TMJs from PBS control MMP13$^{OCY-/-}$ vs 0.05 mg MIA WT and 0.10 mg MIA WT mice.

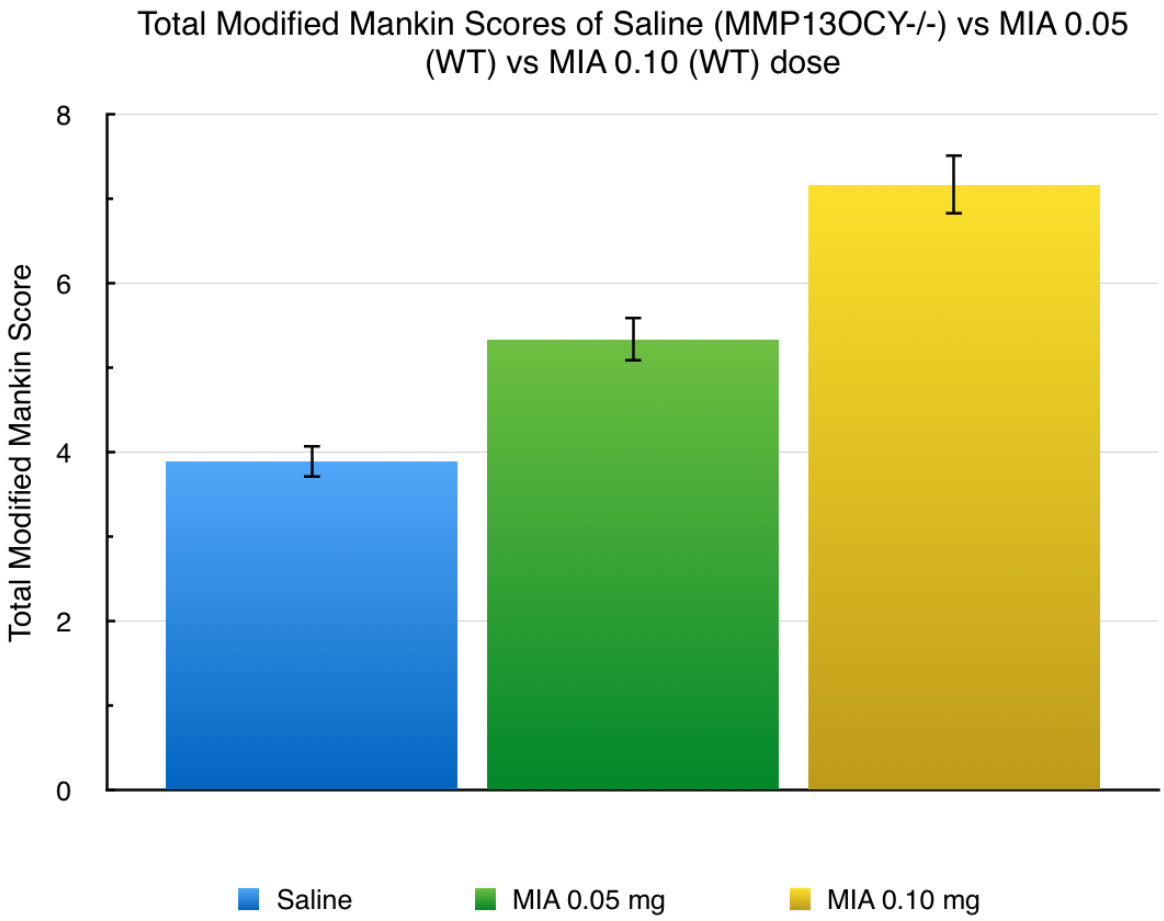

Figure 4.8. Modified Mankin Scores of TMJs from PBS control MMP13$^{OCY-/-}$ vs 0.05 mg MIA WT and 0.10 mg MIA WT mice.

4.4. Histological Observations and Quantitation in WT and MMP13$^{ocy-/-}$ Mice

Figures 4.9 and 4.10 demonstrate coronal sections of male WT and MMP13$^{OCY-/-}$ TMJs at 16 weeks of age (28 dpi controls), that were analyzed via modified Mankin scoring (Figures 4.11 and 4.12). There are visible histological differences between the samples such as the cellular organization in the cartilage layer, the cartilage surface, and the stain intensities. Sample 4 in Figure 4.10 demonstrates superficial fibrillation (black arrow); but does not go so deep as to demonstrates separation of the calcified and uncalcified layers.

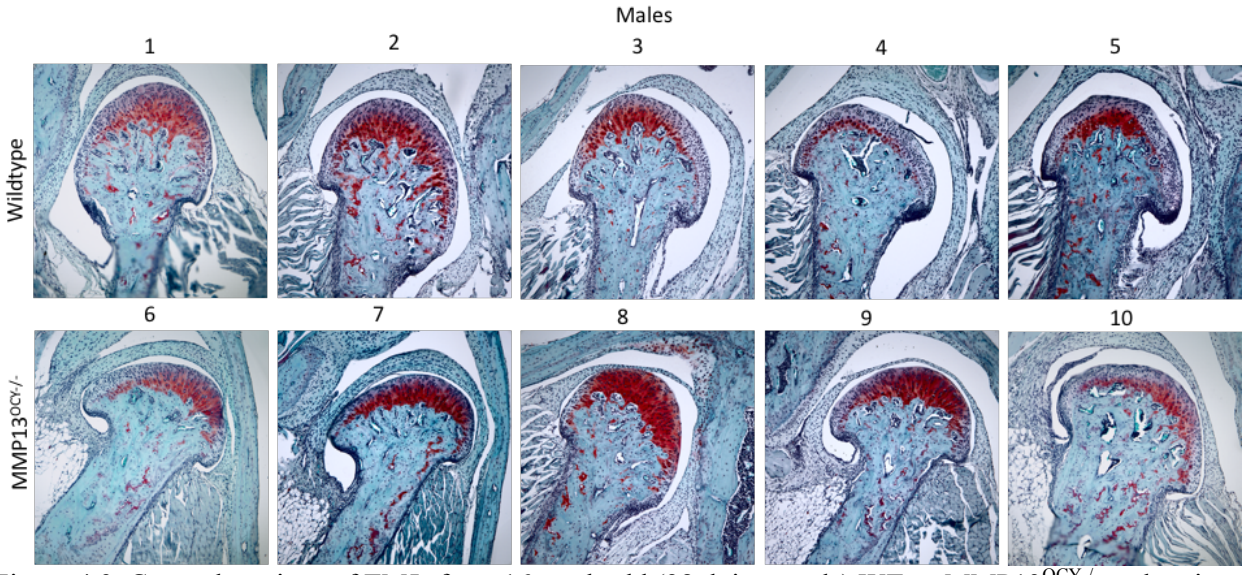

Figure 4.9. Coronal sections of TMJs from 16 week-old (28 dpi controls) WT vs MMP13$^{OCY-/-}$ male mice (10x magnification).

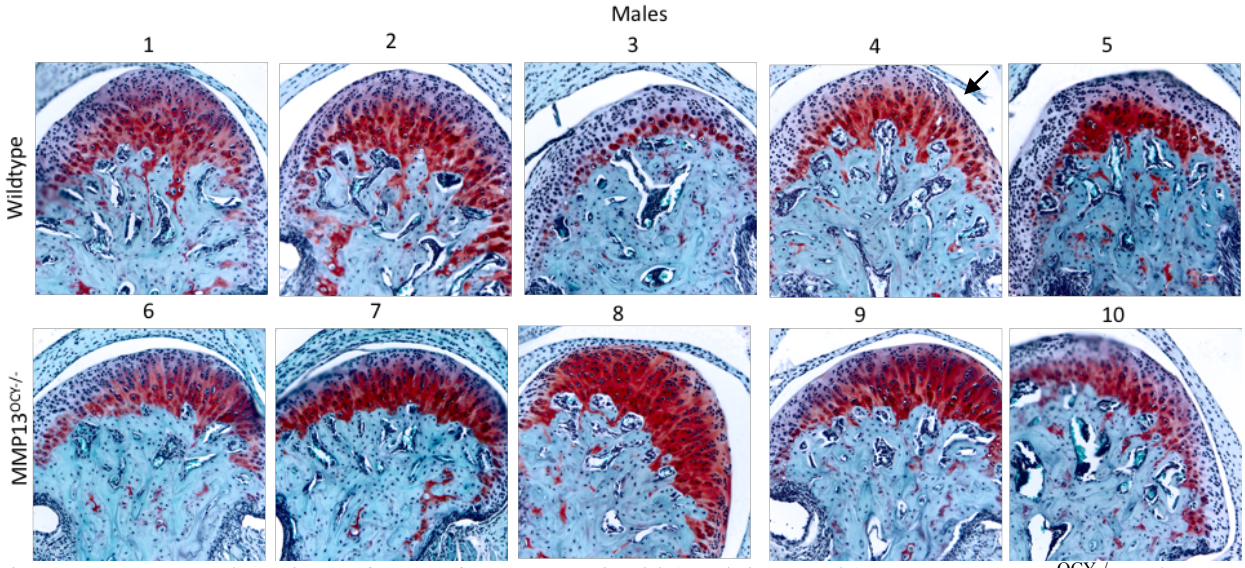

Figure 4.10. Coronal sections of TMJs from 16 week-old (28 dpi controls) WT vs MMP13$^{OCY-/-}$ male mice (20x magnification).

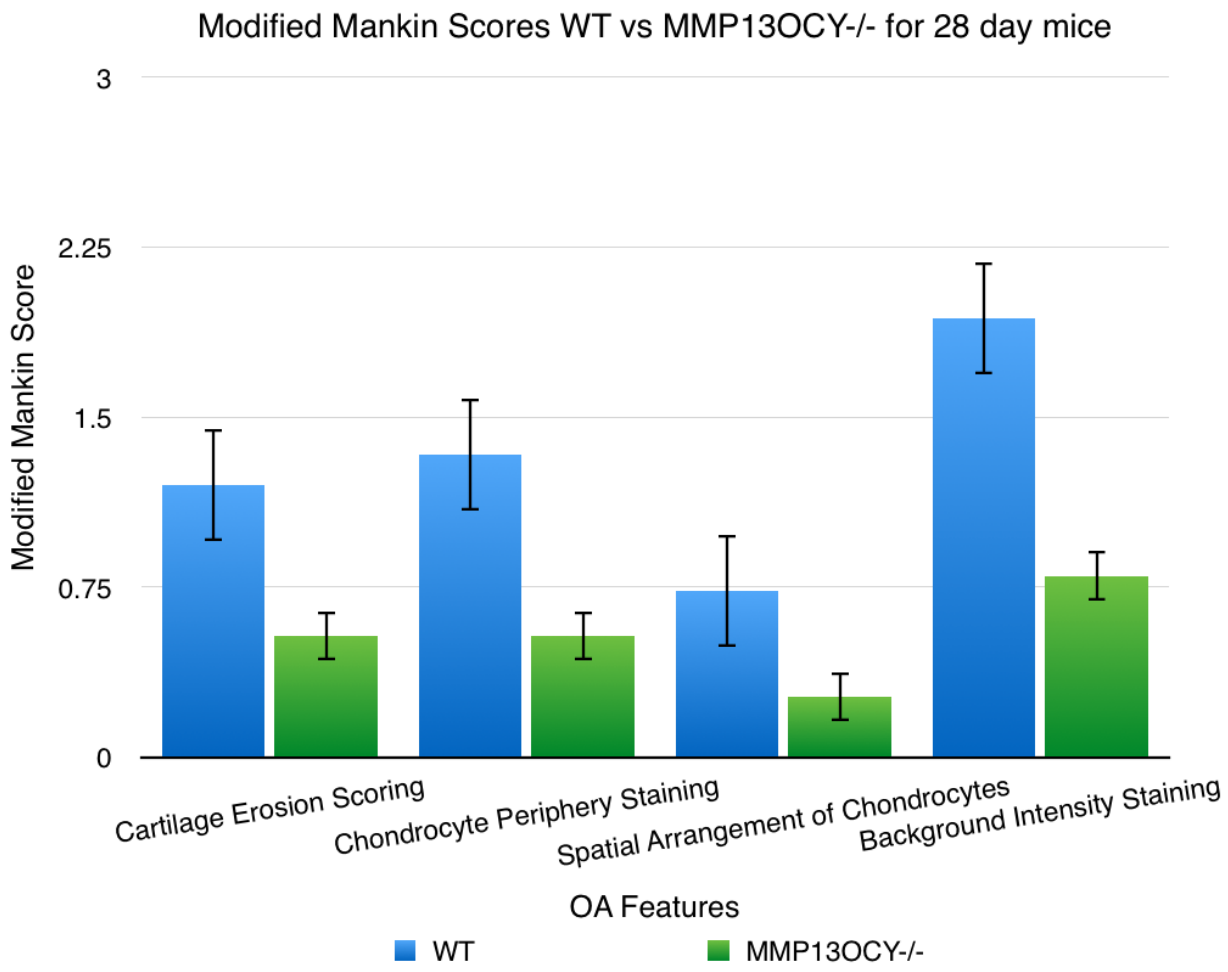

Figure 4.11. Modified Mankin Scores in each of the four histological categories in 16 week-old (28 dpi controls) WT vs MMP13$^{OCY-/-}$ mice.

Figure 4.11 demonstrates the modified Mankin scores in each histological category to be slightly higher than that of the MMP13$^{OCY-/-}$. However there was no statistically significant differences between the two groups ($P<0.05$, two tailed, $t_{crit} = 2.7$) for each of the individual histological categories, which translated to having to accept the null hypothesis. The total Modified Mankin score was also found not to be statistically significantly different between WT and MMP13$^{OCY-/-}$ mice ($P<0.05$, two tailed, $t_{crit} = 2.4$).

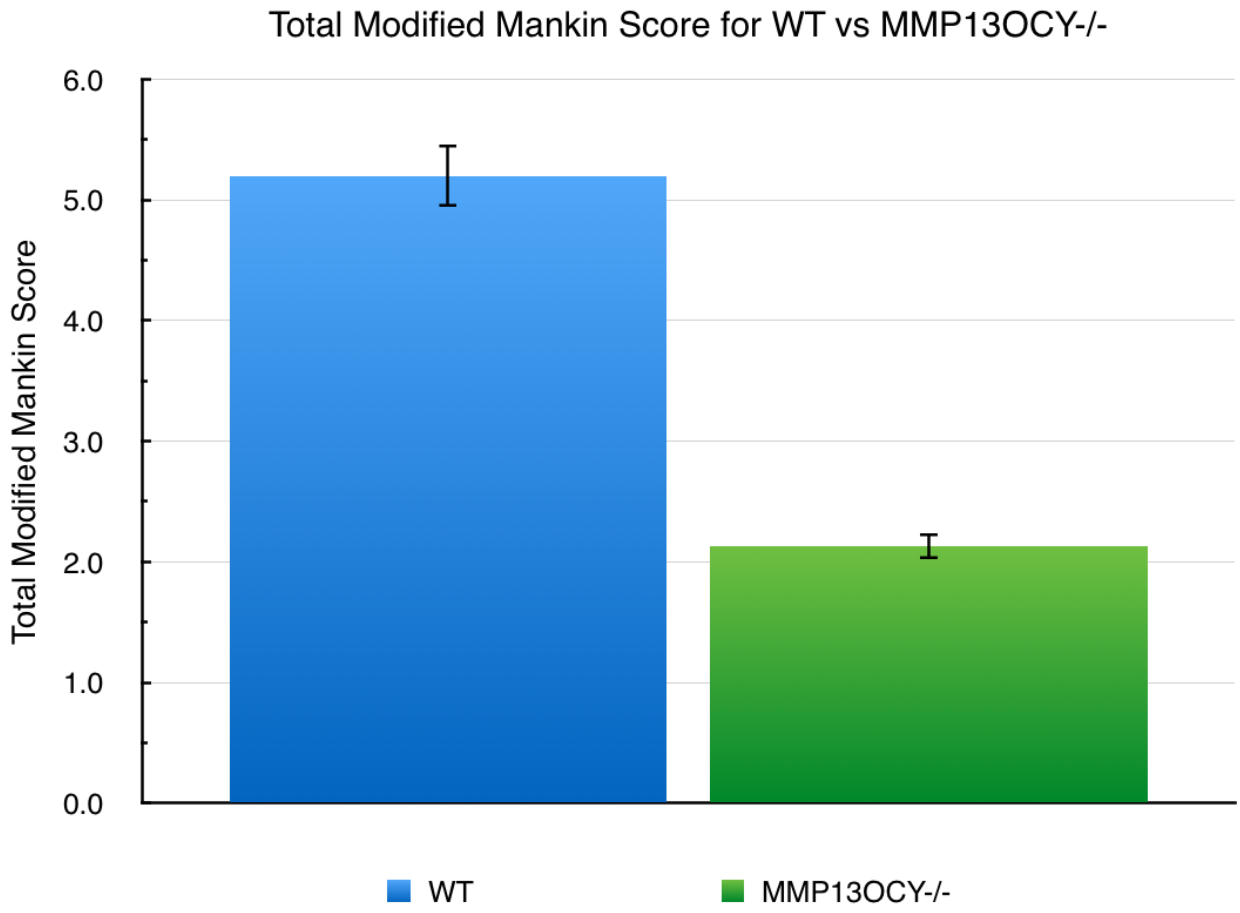

Figure 4.12. Total Modified Mankin Score comparison between 16 week-old (28 dpi controls) WT vs MMP13$^{OCY-/-}$ mice.

CHAPTER 5: DISCUSSION

This study established the foundations for investigation the presentation of OA in WT and $MMP13^{OCY-/-}$ specific to the TMJ. It was postulated that the osteocyte specific MMP13 knockout would result in an increased qualitative expression of OA due to the disorganization the canaliculi projecting from the osteocytes.[3] These canaliculi have been associated with maintenance of bone quality.[12] The direct mechanism is not yet established; however, PLR by virtue of these canaliculi is necessary to achieve bone homeostasis. Because the disorganization of the bony and chondrocytic matrices exposes the structures to degradation which clinically presents in the TMJ degeneration or osteoarthritis, it is expected that these studies would provide important insights in the role of osteocytes and subchondral bone to TMJ OA initiation and progression.

5.1 Injection and Anesthetic Methods

The initial portion of this study was aimed at elucidating the most effective and reliable method for intraarticular injection in order to use a chemically-mediated injury model of OA in the mouse TMJ. Previous studies have injected rabbit, rat or pig TMJs; however, this is the first study to demonstrate consistent intraarticular injection into the mice TMJ.[29–31] This goal presented a multitude of difficulties. Some included the small size of the animal, the inability to find an effective anesthetic dose, as well as the differing anatomy of different age groups of the mice.

To ensure reproducible and predictable OA induction that requires intraarticular delivery of MIA into the TMJ, we utilized the administration of Fast Green dye into the putative location of TMJ as described previously.[25] A series of trials with different approaches of accessing and depositing the dye were undertaken starting with mouse heads to live mice under ketamine/xylazine injectable anesthetic to optimize intra-articular injections of fast green dye. Anesthetized mice were euthanized post-injection via lethal dose of CO_2, followed by cervical dislocation. The goal of these trials was to determine optimal access, precise location and volume of agent to be delivered. Intra-articular administration of the dye was

confirmed by TMJ dissection as demonstrated in Figure 3.1C. This work serves as an important springboard for undertaking future studies to establish temporal dependent outcomes with MIA in using osteocyte-specific MMP13 null mice.

Initial methods involved injection from an infero-superior aspect using the masseter and posterior border of the mouse mandible as an anterior limit. The difficulty in using the injection direction was determining the vertical depth and medial to lateral depth of the TMJ with which to insert the needle. Too deep a vertical depth resulted in piercing of the temporal bone into the and death of the animal. Too lateral of an injection resulted in ineffective injection of the dye into the joint. The dye in this scenario would seep into the adjacent fascial tissue and did not reach the desired TMJ capsule location. This method was slightly more effective in younger mice that we anticipated using because the condyle tends to be more upright, and if a sufficient medial depth was realized without encroaching on the brain tissue, successful injection was achieved. However, after confirming this method of injection, transitioning to older mice to be used in our study resulted in poor injection success. Upon further investigation of the mouse anatomy as well as general growth, it was concluded that the condyle grows in an up and back direction.[38] That is, using the vertical injection method on the correct aged mice resulted in completely missing the condyle due to the now posteriorly displaced location of the condyle. Using a group of correctly aged mice, a new injection protocol was devised.

An additional difficulty was ensuring adequate depth of anesthesia for the mice. Using an inhalant method of anesthesia necessitates having a nose cone placed over the animal's nasal portion to deliver the gas. However, this impeded the eventual selected method of injection as described in the Methods section. Furthermore, due to variabilities in gender and genetic line, the mice required different doses of anesthetic to achieve proper anesthetic depth to not feel the injection. Due to these difficulties, it was eventually decided to use an injectable form of anesthetic; a ketamine/xylazine formulation to allow for adequate anesthetic depth and one that did not impede the mode of injection. Once the proper anesthetic doses were ascertained, determination of the best injection method was resumed.

Another approach used was from a direct anterior approach. The medial border was essentially the maxillary buccal bone region. Care was taken to inject as medial as possible so as to not bypass the TMJ capsule from a lateral aspect. The superior limit was directly inferior to the zygomatic arch. The last variable that is allotted for was the depth of needle injection. Through various attempts it was determined that encountering bone and then depositing the dye presented the most consistent results. The portion of bone that was encountered could either be the posterior wall of the glenoid fossa; or the direct frontal surface of the condylar head. At either of these injection points the deposition of the dye would logically allow for the dye to seep into the compartment and stain the condylar head. This presented about a 70-80% success rate of injection through repeated trials and it was determined to be the most reliable method of injection. As pointed out later in Chapter 6, Future Directions, independent studies can be undertaken to determine truly the most effective means of injection. Additionally, the only current method of confirming injection other than upon final analysis includes premature euthanization and gross dissection to confirm uptake of the dye at the condylar head. Using fluorescent tracers or x-ray methods during injection can lend to greater confidence for injection other than waiting for the end of the experiment to confirm injection success.

5.2 Rationale for Specific Mouse Line

The use of this mouse line for this study allows for setting the foundation of future determinations of the relationship between PLR, cartilage breakdown and OA. Rather than using a global MMP13 knockout, this specific line has suppression of MMP13 only at the osteocyte level. This is to ensure that conclusions drawn regarding the cartilage degradation of the TMJ can be attributed specifically to that of the MMP13 knockout in osteocytes. Furthermore, the destruction in the cartilage with a loss of MMP13 in osteocytes demonstrates the relationship between bone and its overlying cartilage. In a concurrent study run within the lab, osteocyte-specific MMP13 ablation increased trabecular bone mass and disrupted canalicular and collagen organization. Systemic ablation caused decreased post yield deflection and decreased fracture toughness, while osteocyte specific knockout mice demonstrated changes to

cortical bone stiffness and ultimate strength only.[39] Finally, the value in investigating this mouse line was because it allows for a gene knockout whose effects mimic the ingestion or administration of exogenous steroids that are sometimes used for suppression of inflammation in OA therapy.

5.3 The Modified Mankin Scoring

Severity of OA was assessed using a common scoring tool - Mankin scoring. The general scoring protocol was modified for the purposes of this study in only the 'Chondrocyte Periphery Staining' category.[37] The original paper describes an increase in peripheral intensity staining for OA; whereas all samples in this study demonstrated a normal to decreased staining intensity. Normal staining intensity was given a score of '0,' slightly decreased was '1,' and intensely decreased was '2.' The independent graders were calibrated and reviewed various features of OA in order to achieve a consistent assessment of the photomicrographs. Grades that presented with a different of more than two points were re-graded until they were within two points. These scores were averaged and the sum total of the modified Mankin score was used for statistics. Normalcy of the data was assumed, as well as ensuring the test was for independent, two tailed groups. With a larger sample size, the more ideal statistical measure would have been the Mann-Whitney test because it allows for non-normal data.

Cartilage erosion scoring and cartilage periphery staining was determined by examining the border outline of the condylar head. Periphery staining was assessed by ascertaining if the border of the condyle demonstrated a normal amount of safranin dye as compared to the rest of the cartilage layer; or if it presented as slightly or intensely decreased.

Spatial arrangement of the chondrocytes was scored based of the organization and quality of the chondrocytes. For example, the left panel 1 of Figures 4.3 to 4.6 for 0.10 mg MIA WT demonstrates an absolute loss of cellularity and disorganization of the cells. In comparison, panel 2 of Figure 16 for the WT row shows a generally normal pattern of chondrocyte proliferation with stacked cells. Background

staining intensity was assessed by viewing the uptake of safranin along the cartilage layer which varied from a pale pink to an intense, normal red.

5.4. Histologic Findings of the Effects of MIA on the TMJ

Figures 4.3 to 4.7 demonstrate that as a whole, the MIA 0.10 mg dose mice resulted in the greatest severity of OA features. While the current small sample prevents the derivation of valid statistics, with additional samples greater weight can be added to these initial findings. Furthermore, the obvious loss of cells at the condylar level demonstrate the effectiveness of MIA as an injury model for OA. The only trend difference observed in Figure 4.7 is the scores for cartilage erosion scoring. Further sub-analysis can be done for this category once a sufficient *n* is achieved. Our results are consistent with other studies using MIA as a method for OA induction – even with different animals and different locations. For example, punctuate allodynia and weight bearing deficits in rats injected with MIA has been demonstrated for up to 10 weeks and was able to be reversed with pain medications.[18] Similarly, our foundational paper demonstrated that OA-inducing effects of MIA on rat TMJs can be observed within just a few days.[25] Knee OA has also been induced with MIA in rabbits – with characteristic lesions presenting such as thickening and fibrillation. MIA has been used previously as a chemical method to induce OA and serves great value as a models for future studies.

5.5 OA Phenotype in WT and MMP13OCY$^{-/-}$ Mice

Modified Mankin scoring for the WT and MMP13$^{OCY-/-}$ in Figure 4.2 demonstrates that the mean scores from graders were higher in the WT animals than in MMP13$^{OCY-/-}$ mice. While this is an unexpected finding, the differences were not statistically between the two groups. It is plausible that the sample size was underpowered and that additional samples with a more consistent protocol could allow for further confirmation of this conclusion. A two sample paired *t* test was utilized to compare individual categories as well as the total Mankin score. The *t* values obtained for cartilage erosion, chondrocyte periphery staining, spatial arrangement of chondrocytes, and background staining intensity was 0.059, 0.009, 0.101,

and 0.005, respectively ($P<0.05$, df = 4, $t_{crit} = 2.7$). For the total Mankin score $t_{crit} = 2.4$ with the $t = 0.030$. In all cases the null was unable to be rejected. The largest culprit in this inability is likely the small sample size that does not allow for a smaller t_{crit} value. If with further samples statistically significant greater OA scores are found in WT than MMP13 null mice, this would warrant further investigation as to possible mechanisms of spontaneous OA in WT mice and the protective effect of the absence of MMP13 in osteocytes in mitigating this OA. Possible suggestions include that the absence of the MMP13 in osteocytes could lead to upregulation of other MMPs to ensure homeostasis of the condylar tissues.

CHAPTER 6: FUTURE DIRECTIONS

The proposed studies will serve as a foundation for long term investigations that include determining the basis by which defects in osteocyte matrix remodeling affect the function of the fibrocartilage-bone complex. To go to the beginning of the study, a new study can be stemmed simply from the injection protocol. Various methods were analyzed for this study and the most predictable method of injection was chosen. However, a variety of methods and techniques have been presented in the literature for larger animals. In this study, using a smaller animal for the purposes of using the specific genetic line of mice presented a new challenge in exploring the best method of injection as well as induction of anesthesia. Exploring these avenues in studies devoted solely to each individual task would heighten the confidence in the conclusions drawn from each respective study. This study explored a single gender within a single time point between WT and MMP13$^{OCY-/-}$. This study sets up the basis for future studies to include both sexes, in addition to multiple time points. Furthermore, addition of more samples would allow for greater ability to distinguish between inherent variability of such studies and actual significant differences between the two animal groups. Although histologic observations showed substantial differences between the control and the different MIA dosage groups, increasing the sample size for this determination would add to the robustness of the study.

Additionally, including other quantitative parameters to measure the differences in chondrocyte presence and quality can be performed in the future on this sample collected from this study as well as the additional animals that could be included. Another dimension of analysis to include for this study is μCT analysis. While current methods of μCT analysis are well demarcated for mice knee OA or OA for larger animals, studying mice TMJs present additional challenges due to the very small size of tissues. While μCT analysis was attempted for this study, several difficulties were encountered in the process of attempting to do the analysis. Firstly, the parameters to obtain a high quality image for analysis were difficult to identify. A high quality image of the condyle is necessary in order to demarcate the superficial

condylar layer from the trabecular bone. Additionally, the thickness of this layer is variable throughout the condyle. While a computer program is able to extrapolate estimates of this layer from a starting, midpoint, and final region of interest – the exact thickness is unknown. Follow up work with a lab conversant with μCT analyses of TMJs are currently being pursued.

In the longer term, we intend to decipher whether the progression and severity of OA in response to subchondral bone defects are different between joints with hyaline articular cartilage versus the fibrocartilage-lined TMJ. Additional future directions of study include testing the ability of molecular interventions that rescue osteocyte function to mitigate the severity of TMJ OA. Thus, the work in this study, as well as in future proposals will establish the model system and show proof of concept for the role of osteocytes in TMJ disease, providing the foundation needed for future studies intended to identify new therapeutic interventions. Finally, the data collected from this study will be critical to seeking NIH funding to undertake more thorough mechanistic studies on the interactions between subchondral bone and fibrocartilage in contributing to progression of OA and the specificity of this response to the TMJ as opposed do appendicular hyaline cartilage joints.

CHAPTER 7: CONCLUSIONS

7.1 Injection and Anesthetic Method

Through the various attempts from this study, it can be concluded that the most predictable method of injection is from an anterior aspect, as medial as possible, directly inferior to the zygomatic process. The depth limiting factor is the needle tip encountering bone.

7.2 WT vs MMP13$^{OCY-/-}$

Based on the statistical analysis, we are unable to reject the null hypothesis and conclude that there is no difference between the osteoarthritic features of the WT vs MMP13$^{OCY-/-}$ mice at 12 to 16 weeks of age. This conclusion can be further affirmed by future studies, further calibration of the injection protocol, and increasing the sample size.

7.3 MIA Dosage

From the observable OA characteristics in the TMJ at 0.10 mg MIA dose, it can be concluded for future studies that this is an effective dose to successfully induce OA. Since there appears to be an effect at 0.05 mg MIA dose, this lower dose may be useful in providing more dynamic range in the severity of injury induced OA to discern the combined effects of genotype and injury on TMJ OA.

REFERENCES

1. Das SK. TMJ osteoarthritis and early diagnosis. *J Oral Biol Craniofacial Res*. 2013. doi:10.1016/j.jobcr.2013.10.003

2. Ozeki N, Kawai R, Yamaguchi H, et al. IL-1β-induced matrix metalloproteinase-13 is activated by a disintegrin and metalloprotease-28-regulated proliferation of human osteoblast-like cells. *Exp Cell Res*. 2014. doi:10.1016/j.yexcr.2014.02.018

3. Fowler TW, Acevedo C, Mazur CM, et al. Glucocorticoid suppression of osteocyte perilacunar remodeling is associated with subchondral bone degeneration in osteonecrosis. *Sci Rep*. 2017. doi:10.1038/srep44618

4. Cheatle MD, Wasser T, Foster C, Olugbodi A, Bryan J. Prevalence of suicidal ideation in patients with chronic non-cancer pain referred to a behaviorally based pain program. *Pain Physician*. 2014.

5. Zingg M, Iizuka T, Geering AH, Raveh J. Degenerative temporomandibular joint disease: surgical treatment and long-term results. *J Oral Maxillofac Surg*. 1994.

6. Wadhwa S, Kapila S. TMJ disorders: future innovations in diagnostics and therapeutics. *J Dent Educ*. 2008. doi:72/8/930 [pii]

7. Van Doren SR. Matrix metalloproteinase interactions with collagen and elastin. *Matrix Biol*. 2015. doi:10.1016/j.matbio.2015.01.005

8. Bellido M, Lugo L, Roman-Blas JA, et al. Subchondral bone microstructural damage by increased remodelling aggravates experimental osteoarthritis preceded by osteoporosis. *Arthritis Res Ther*. 2010. doi:10.1186/ar3103

9. Cevidanes LHS, Walker D, Schilling J, et al. 3D osteoarthritic changes in TMJ condylar morphology correlates with specific systemic and local biomarkers of disease. *Osteoarthr Cartil*.

2014. doi:10.1016/j.joca.2014.06.014

10. Karsdal MA, Madsen SH, Christiansen C, Henriksen K, Fosang AJ, Sondergaard BC. Cartilage degradation is fully reversible in the presence of aggrecanase but not matrix metalloproteinase activity. *Arthritis Res Ther*. 2008. doi:10.1186/ar2434

11. Shi J, Lee S, Pan HC, et al. Association of Condylar Bone Quality with TMJ Osteoarthritis. *J Dent Res*. 2017. doi:10.1177/0022034517707515

12. Tang SY, Herber RP, Ho SP, Alliston T. Matrix metalloproteinase-13 is required for osteocytic perilacunar remodeling and maintains bone fracture resistance. *J Bone Miner Res*. 2012. doi:10.1002/jbmr.1646

13. Ramaesh T, Bard JBL. The growth and morphogenesis of the early mouse mandible: A quantitative analysis. *J Anat*. 2003. doi:10.1046/j.1469-7580.2003.00210.x

14. Murakami T, Fukunaga T, Takeshita N, et al. Expression of Ten-m/Odz3 in the fibrous layer of mandibular condylar cartilage during postnatal growth in mice. *J Anat*. 2010. doi:10.1111/j.1469-7580.2010.01267.x

15. Gepstein A, Arbel G, Blumenfeld I, Peled M, Livne E. Association of metalloproteinases, tissue inhibitors of matrix metalloproteinases, and proteoglycans with development, aging, and osteoarthritis processes in mouse temporomandibular joint. *Histochem Cell Biol*. 2003. doi:10.1007/s00418-003-0544-1

16. Liang W, Li X, Gao B, et al. Observing the development of the temporomandibular joint in embryonic and post-natal mice using various staining methods. *Exp Ther Med*. 2016. doi:10.3892/etm.2015.2937

17. Ohshima T, Yonezu H, Nishibori Y, Uchiyama T, Shibahara T. Morphological Observation of

Process of Mouse Temporomandibular Joint Formation. *Bull Tokyo Dent Coll*. 2011. doi:10.2209/tdcpublication.52.183

18. Combe R, Bramwell S, Field MJ. The monosodium iodoacetate model of osteoarthritis: A model of chronic nociceptive pain in rats? *Neurosci Lett*. 2004. doi:10.1016/j.neulet.2004.08.023

19. Bendele A. Animal models of rheumatoid arthritis. *J Musculoskelet Neuronal Interact*. 2001. doi:10.1002/eji.200939578

20. Cledes G, Felizardo R, Foucart JM, Carpentier P. Validation of a chemical osteoarthritis model in rabbit temporomandibular joint: a compliment to biomechanical models. *Int J Oral Maxillofac Surg*. 2006. doi:10.1016/j.ijom.2006.05.003

21. Güler N, Kürkü M, Duygu G, Am B. Sodium iodoacetate induced osteoarthrosis model in rabbit temporomandibular joint: CT and histological study (Part I). *Int J Oral Maxillofac Surg*. 2011. doi:10.1016/j.ijom.2011.07.908

22. Kobayashi K, Imaizumi R, Sumichika H, et al. Sodium iodoacetate-induced experimental osteoarthritis and associated pain model in rats. *J Vet Med Sci*. 2003. doi:10.1292/jvms.65.1195

23. Ikeda Y, Yonemitsu I, Takei M, Shibata S, Ono T. Mechanical loading leads to osteoarthritis-like changes in the hypofunctional temporomandibular joint in rats. *Arch Oral Biol*. 2014. doi:10.1016/j.archoralbio.2014.08.010

24. Matias EMC, Mecham DK, Black CS, et al. Malocclusion model of temporomandibular joint osteoarthritis in mice with and without receptor for advanced glycation end products. *Arch Oral Biol*. 2016. doi:10.1016/j.archoralbio.2016.05.007

25. Wang XD, Kou XX, He DQ, et al. Progression of Cartilage Degradation, Bone Resorption and Pain in Rat Temporomandibular Joint Osteoarthritis Induced by Injection of Iodoacetate. *PLoS*

One. 2012. doi:10.1371/journal.pone.0045036

26. Tavakkoli-Jou M, Miller AJ, Kapila S. Mandibulofacial Adaptations in a Juvenile Animal Model of Temporomandibular Joint Arthritis. *J Dent Res*. 1999. doi:10.1177/00220345990780080801

27. Goldring SR, Goldring MB. Changes in the osteochondral unit during osteoarthritis: Structure, function and cartilage bone crosstalk. *Nat Rev Rheumatol*. 2016. doi:10.1038/nrrheum.2016.148

28. Goldring MB, Goldring SR. Articular cartilage and subchondral bone in the pathogenesis of osteoarthritis. In: *Annals of the New York Academy of Sciences*. ; 2010. doi:10.1111/j.1749-6632.2009.05240.x

29. Weinstein RS. Glucocorticoid-Induced Bone Disease. In: *Primer on the Metabolic Bone Diseases and Disorders of Mineral Metabolism: Eighth Edition*. ; 2013. doi:10.1002/9781118453926.ch58

30. Kamekura S, Hoshi K, Shimoaka T, et al. Osteoarthritis development in novel experimental mouse models induced by knee joint instability. *Osteoarthr Cartil*. 2005. doi:10.1016/j.joca.2005.03.004

31. Sampson ER, Beck CA, Ketz J, et al. Establishment of an index with increased sensitivity for assessing murine arthritis. *J Orthop Res*. 2011. doi:10.1002/jor.21368

32. Kapila S, Tavakkoli Jou MR, Lee C, Miller AJ, Richards DW. Development and Histologic Characterization of an Animal Model of Antigen-induced Arthritis of the Juvenile Rabbit Temporomandibular Joint. *J Dent Res*. 1995. doi:10.1177/00220345950740121001

33. Stickens D. Altered endochondral bone development in matrix metalloproteinase 13-deficient mice. *Development*. 2004. doi:10.1242/dev.01461

34. Lu Y, Xie Y, Zhang S, Dusevich V, Bonewald LF, Feng JQ. DMP1 -Targeted Cre expression in odontoblasts and osteocytes. *J Dent Res*. 2007. doi:10.1177/154405910708600404

35. Tanaka E, Detamore MS, Mercuri LG. Degenerative Disorders of the Temporomandibular Joint: Etiology, Diagnosis, and Treatment. *J Dent Res*. 2008. doi:10.1177/154405910808700406

36. van der Sluijs JA, Geesink RGT, van der Linden AJ, Bulstra SK, Kuyer R, Drukker J. The reliability of the mankin score for osteoarthritis. *J Orthop Res*. 1992. doi:10.1002/jor.1100100107

37. Matías EMC, Mecham DK, Black CS, et al. Malocclusion model of temporomandibular joint osteoarthritis in mice with and without receptor for advanced glycation end products. *Arch Oral Biol*. 2016. doi:10.1016/j.archoralbio.2016.05.007

38. Mashiatulla M, Moran MM, Chan D, et al. Murine articular cartilage morphology and compositional quantification with high resolution cationic contrast-enhanced μCT. *J Orthop Res*. 2017. doi:10.1002/jor.23595

39. Mazur CM, Woo JJ, Yee CS, et al. Suppressed Osteocyte Perilacunar / Canalicular Remodeling Plays a Causal Role in Osteoarthritis. *bioRxiv*. 2019. doi:10.1101/534768

Publishing Agreement

It is the policy of the University to encourage the distribution of all theses, dissertations, and manuscripts. Copies of all UCSF theses, dissertations, and manuscripts will be routed to the library via the Graduate Division. The library will make all theses, dissertations, and manuscripts accessible to the public and will preserve these to the best of their abilities, in perpetuity.

Please sign the following statement:

I hereby grant permission to the Graduate Division of the University of California, San Francisco to release copies of my thesis, dissertation, or manuscript to the Campus Library to provide access and preservation, in whole or in part, in perpetuity.

Author Signature

5/28/2019

Date